ผลของการเติมโพแทสเซียมและอัตราส่วนของซิลิกาต่ออะลูมินาต่อการผลิตกรดอะคริลิก
จากกรดแลคติกบนตัวเร่งปฏิกิริยาซีโอไลต์เบต้า

นายวีรพงษ์ ภูไชยแสง

วิทยานิพนธ์นี้เป็นส่วนหนึ่งของการศึกษาตามหลักสูตรปริญญาวิศวกรรมศาสตรมหาบัณฑิต
สาขาวิชาวิศวกรรมเคมี ภาควิชาวิศวกรรมเคมี
คณะวิศวกรรมศาสตร์ จุฬาลงกรณ์มหาวิทยาลัย
ปีการศึกษา 2559

THE EFFECT OF POTASSIUM ADDITION AND SiO_2/Al_2O_3 RATIOS ON ACRYLIC ACID PRODUCTION FROM LACTIC ACID ON BETA ZEOLITE CATALYST

Mr. Weerapong Phochaisang

A Thesis Submitted in Partial Fulfillment of the Requirements
for the Degree of Master of Engineering Program in Chemical Engineering
Department of Chemical Engineering
Faculty of Engineering
Chulalongkorn University
Academic Year 2016

Thesis Title	THE EFFECT OF POTASSIUM ADDITION AND SiO_2/Al_2O_3 RATIOS ON ACRYLIC ACIDPRODUCTION FROM LACTIC ACID ON BETA ZEOLITE CATALYST
By	Mr. Weerapong Phochaisang
Field of Study	Chemical Engineering
Thesis Advisor	Assistant Professor Suphot Phatanasri, D.Eng.

Accepted by the Faculty of Engineering, Chulalongkorn University in Partial Fulfillment of the Requirements for the Master's Degree

.....Dean of the Faculty of Engineering

(Associate Professor Supot Teachavorasinskun, D.Eng.)

THESIS COMMITTEE

.....Chairman

(Associate Professor Joongjai Panpranot, Ph.D.)

.....Thesis Advisor

(Assistant Professor Suphot Phatanasri, D.Eng.)

.....Examiner

(Palang Bumroongsakulsawat, Ph.D.)

.....External Examiner

(Assistant Professor Soipatta Soisuwan, D.Eng.)

วีรพงษ์ ภูไชยแสง : ผลของการเติมโพแทสเซียมและอัตราส่วนของซิลิกาต่ออะลูมินาต่อการผลิตกรดอะคริลิกจากกรดแลคติกบนตัวเร่งปฏิกิริยาซีโอไลต์เบต้า (THE EFFECT OF POTASSIUM ADDITION AND SiO_2/Al_2O_3 RATIOS ON ACRYLIC ACIDPRODUCTION FROM LACTIC ACID ON BETA ZEOLITE CATALYST) อ.ที่ปรึกษาวิทยานิพนธ์หลัก: ผศ. ดร. สุพจน์ พัฒนะศรี, 81 หน้า.

ในงานวิจัยนี้ได้ทำการศึกษาผลของการเติมโพแทสเซียมลงบนตัวเร่งปฏิกิริยาซีโอไลต์เบต้าด้วยอัตราส่วน 2, 4 และ 6 เปอร์เซ็นต์ โดยน้ำหนัก โดยวิธีการเคลือบฝังแบบเปียก และผลของอัตราส่วนซิลิกาต่ออะลูมินาบนตัวเร่งปฏิกิริยาซีโอไลต์เบต้าต่อความสามารถในการเร่งปฏิกิริยาดีไฮเดรชันของกรดแลคติกเพื่อผลิตกรดอะคริลิค จากการวิเคราะห์ด้วยเทคนิคการคายซับแก๊สแอมโมเนีย (NH_3-TPD) และการคายซับแก๊สคาร์บอนไดออกไซด์ (CO_2-TPD) พบว่าการเติมโพแทสเซียมจะช่วยลดความเป็นกรดและช่วยเพิ่มความเป็นเบสให้กับตัวเร่งปฏิกิริยาซีโอไลต์เบต้าได้ แต่ในขณะเดียวกันจากการวิคราะห์ด้วยเทคนิคการกระเจิงของรังสีเอ็กซ์ (X-Ray Diffraction) พบว่าการเติมโพแทสเซียมก็ส่งผลทำให้เกิดการทำลายต่อโครงสร้างผลึกของตัวเร่งปฏิกิริยาซีโอไลต์เบต้าเช่นเดียวกัน ในส่วนของผลอัตราส่วนของซิลิกาต่ออะลูมินา พบว่าการเพิ่มขึ้นของอัตราส่วนของซิลิกาต่ออะลูมินา จะช่วยลดความเป็นกรดของตัวเร่งปฏิกิริยาซีโอไลต์เบต้า แต่ในขณะเดียวกันความเป็นผลึกของตัวเร่งปฏิกิริยาก็มีค่าลดลงเช่นเดียวกัน ตัวเร่งปฏิกิริยาซีโอไลต์เบต้าที่เติมด้วยโพแทสเซียม 4 เปอร์เซ็นโดยน้ำหนักและมีอัตราส่วนซิลิกาต่ออะลูมินาเป็น 360 มีความสามารถในการเร่งปฏิกิริยาได้ดีที่สุดโดยแสดงค่าร้อยละการเปลี่ยนแปลงของกรดแลคติกและค่าการเลือกเกิดกรดอะคริลิคที่สูงที่สุด คือ 100 เปอร์เซ็นต์การเปลี่ยนแปลงกรดแลคติกและ 43.8 เปอร์เซ็นต์การเลือกเกิดกรดคริลิค เนื่องจากมีคุณสมบัติความเป็นกรดและเบสที่เหมาะสมในการเกิดปฏิกิริยา นอกจากยังพบว่าการเติมโพแทสเซียมยังช่วยปรับปรุงคุณสมบัติทางความร้อนของตัวเร่งปฏิกิริยาซีโอไลต์เบต้าได้

ภาควิชา วิศวกรรมเคมี ลายมือชื่อนิสิต .....

สาขาวิชา วิศวกรรมเคมี ลายมือชื่อ อ.ที่ปรึกษาหลัก .....

ปีการศึกษา 2559

5770465721 : MAJOR CHEMICAL ENGINEERING

KEYWORDS: H-BETA ZEOLITE / POTASSIUM / SIO2/AL2O3 RATIO / ACIDITY / BASICITY / LACTIC ACID DEHYDRATION

WEERAPONG PHOCHAISANG: THE EFFECT OF POTASSIUM ADDITION AND SiO_2/Al_2O_3 RATIOS ON ACRYLIC ACIDPRODUCTION FROM LACTIC ACID ON BETA ZEOLITE CATALYST. ADVISOR: ASST. PROF. SUPHOT PHATANASRI, D.Eng., 81 pp.

In this research, the effect of potassium loading on H-beta zeolite catalysts with 2, 4 and 6 wt% prepared via incipient wetness impregnation method was studied. Furthermore, the effect of SiO_2/Al_2O_3 ratios of H-beta zeolite catalysts was also investigated. The catalytic performances of all the catalysts were tested on dehydration of lactic acid to acrylic acid. The NH_3-TPD and CO_2-TPD results demonstrated the decrease of acid property and increase of basic property of H-beta zeolite catalysts when increasing potassium loading. In addition, the XRD result showed that the crystallinity structure of H-beta zeolite tends to be destroyed when increasing potassium loading. As for, the effect of SiO_2/Al_2O_3 ratios of H-beta zeolite catalysts, the increase of SiO_2/Al_2O_3 ratio tends to decrease acid properties of H-beta zeolite catalysts. Furthermore, the crystallinity structure of catalysts also decreased. As well, the H-beta zeolite catalyst with potassium loading of 4 wt% and SiO_2/Al_2O_3 ratio of 360 exhibited the highest catalytic performance due to its suitably moderated acid and base properties. Such catalyst demonstrated the highest lactic acid conversion and acrylic acid selectivity with 100% lactic acid conversion and 43.8% acrylic acid selectivity. Moreover, the modification of H-beta zeolite with potassium can improve the durability of catalysts during lactic acid dehydration reaction.

Department: Chemical Engineering Student's Signature .....

Field of Study: Chemical Engineering Advisor's Signature .....

Academic Year: 2016

ACKNOWLEDGEMENTS

First of all, the author would like to express his gratitude and appreciation to his advisor, Assistant Professor Dr. Suphot Phatanasri for the valuable suggestion, stimulation, useful discussion and knowledge for this research. The author would also be grateful to Associate Professor Joongjai Panpranot, as the chairman, Dr. Palang Bumroongsakulsawat and Assistant Professor Soipatta Soisuwan as the members of the thesis committee.

Furthermore, the author is indebted to the kind suggestions and useful help of Mr. Kijchai Karnjanaprapakul from Faculty of Engineering, Chulalongkorn University and Mr. Chompupol Sanyonk from Global R&D company, who always suggest how to put in place for the completion of reaction line assembly. The special thanks also go to all friends in Center of Excellence on catalysis and catalytic Reaction Engineering for their useful assistance and encouragement.

Finally, the author would like to dedicate any achievement of this work to his parents, who have always been painstakingly the source of motivation, support encouragement. As well as, the supreme idol to the author.

CONTENTS

Page

THAI ABSTRACT iv

ENGLISH ABSTRACT v

ACKNOWLEDGEMENTS vi

CONTENTS vii

TABLE CONTENTS 11

LIST OF FIGURES 12

CHAPTER I INTRODUCTION 16

1.1 Rationales 16

1.2 Research objective 17

1.3 Research scope 18

1.4 Research and Methodology 19

1.4.1 Part I: The effect of potassium loading on catalytic activity 19

1.4.2 Part II: The effect of SiO_2/Al_2O_3 ratios of H-beta zeolite on catalytic activity 20

CHAPTER II THEORY AND LITERATURE REVIEW 21

2.1 Reactant and Product 21

2.1.1 Lactic acid 21

2.1.2 Acrylic acid 22

2.2 Dehydration reaction of lactic acid to acrylic acid 23

2.2.1 Side reaction in the dehydration reaction of lactic acid 23

2.2.2 The mechanism on heterogeneous catalyst 23

2.2.3 The kinetic of lactic acid dehydration 24

2.3 Zeolite catalyst 25

Page

2.3.1 Structures and definitions 25
2.3.2 Beta zeolites catalysts 26
2.4 Deactivation of catalyst 27
2.4.1 Poisoning 27
2.4.2 Sintering 27
2.4.3 Fouling 28
2.5 Literature review 29
2.5.1 Suitable properties of catalyst for dehydration of lactic acid to acrylic acid. 29
2.5.2 Suitable reaction condition for dehydration of lactic acid to acrylic acid. 31
CHAPTER III EXPERIMENTAL 32
3.1 Preparation of catalyst 32
3.1.1 Chemicals 32
3.1.2 The incipient wetness impregnation method preparation of catalysts 32
3.2 Characterization of Catalyst 33
3.2.1 X-Ray Diffraction (XRD). 33
3.2.2 Nitrogen physisorption (BET) 33
3.2.3 Scanning electron microscopy (SEM) and energy x-ray spectroscopy (EDX) 33
3.2.4 Ammonium temperature programed desorption (NH_3-TPD) 33
3.2.5 Carbon dioxide temperature programed desorption (CO_2-TPD). 33
3.2.6 Thermal gravimetric and differential thermal analysis (TG-DTA). 33
3.3 Dehydration of Lactic Acid Testing. 34

Page

3.3.1 Chemicals and Reactant. 34

3.3.2 Instrument and Apparatus. 34

3.3.3 Dehydration Reaction of Lactic Acid Procedure. 36

CHAPTER IV RESULTS AND DICCUSSION 37

4.1 The effect of potassium loading on catalytic activity 37

4.1.1 Characterization of Catalyst 37

4.1.1.1 Scanning electron microscopy (SEM) and energy x-ray spectroscopy (EDX) 37

4.1.1.2 X-Ray Diffraction (XRD). 39

4.1.1.3 Nitrogen physisorption 40

4.1.1.4 Ammonia temperature-programed desorption (NH_3-TPD) 42

4.1.1.5 Carbondioxide temperature-programed desorption (CO_2-TPD) 44

4.1.1.6 Thermal gravimetric and differential thermal analysis (TG-DTA) 46

4.1.2 Dehydration of Lactic Acid Testing. 47

4.2 The effect of SiO_2/Al_2O_3 ratio of H-beta zeolite to catalytic activity 51

4.2.1 Characterization of Catalyst 51

4.2.1.1 Scanning electron microscopy (SEM) and energy x-ray spectroscopy (EDX) 51

4.2.1.2 X-Ray Diffraction (XRD) 53

4.2.1.3 Nitrogen physisorption 55

4.2.1.4 Ammonia temperature-programmed desorption (NH_3-TPD) 57

4.2.1.5 Carbon dioxide temperature-programmed desorption (CO_2-TPD) 59

4.2.1.6 Thermal gravimetric and differential thermal analysis (TG-DTA) 61

Page

4.2.2 Dehydration of Lactic Acid Testing..... 62
CHAPTER V CONCLUSIONS..... 66
5.1 Conclusions..... 66
5.2 Recommendation..... 67
REFERENCES..... 68
APPENDIX..... 73
APPENDIX A. CALCULATION OF CATALYST PREPARATION..... 74
APPENDIX B. CALCULATION OF THE ACID SITE OF CATALYST..... 75
APPENDIX C. CALCULATION OF THE BASIC SITE OF CATALYST..... 76
APPENDIX D. CALIBRATION CURVE OF REAGENT..... 77
APPENDIX E. CALCULATION OF CONVERTION AND SELECTIVITY..... 80
VITA..... 81

TABLE CONTENTS

Table 2. 1 The chemical and physical properties of lactic acid..... 21

Table 2. 2 The chemical and physical properties of acrylic acid..... 22

Table 2. 3 the kinetic data of lactic acid dehydration 24

Table 3. 1 Operating conditions of gas chromatographs 35

Table 4. 1 The element composition of catalyst from energy X-ray spectroscopy.... 37

Table 4. 2 The physical properties of potassium modified H-beta zeolite catalysts..... 40

Table 4. 3 The acidity properties of H-beta zeolite catalyst and potassium modified H-beta zeolite catalyst..... 42

Table 4. 4 The basicity properties of H-beta zeolite catalyst and potassium modified H-beta zeolite catalyst..... 44

Table 4. 5 The catalytic performance of potassium modified catalysts 48

Table 4. 6 The element composition of modified H-beta zeolite catalysts with potassium loading of 4 wt% from energy X-ray spectroscopy 51

Table 4. 7 The physical properties of modified H-beta zeolite catalysts with potassium loading 4 wt%..... 55

Table 4. 8 The acidity properties of modified H-beta zeolite catalysts with potassium loading 4 wt%..... 57

Table 4. 9 The basicity properties of modified H-beta zeolite catalysts with potassium loading 4 wt%..... 59

Table 4. 10 The catalytic performance of potassium modified catalysts 63

LIST OF FIGURES

Figure 2. 1 Structure of L (+) and D (-) isomers of the lactic acid 21

Figure 2. 2 Oxidation reaction pathway of propylene to acrylic acid (a) Te/VPO and (b) Te–P/NiMoO catalysts 22

Figure 2. 3 Main conversion pathways of lactic acid in the gas phase reaction. 23

Figure 2. 4 The mechanism of lactic acid dehydration to acrylic acid reaction on modified NaY-zeolite catalyst 24

Figure 2. 5 Typical pore diameter distributions of porous solids. 25

Figure 2. 6 Structure of H-beta zeolite 26

Figure 2. 7 The poisoning model during ethylene hydrogenation by sulfur atom at metal surface 27

Figure 2. 8 Two sintering model due to growth of crystallite (A) atomic 27

Figure 2. 9 The fouling model of a supported metal catalyst due to carbon deposition 28

Figure 3. 1 Experimental set-up for reaction test. 34

Figure 4. 1 Potassium distribution on surface of modified H-beta zeolite360 catalysts: (a) Potassium 2wt%K, (b) Potassium 4wt%K and (c) Potassium 6wt%K 38

Figure 4. 2 SEM images of the H-beta zeolite360 and the modified H-beta zeolite360 catalysts: (a) H-beta zeolite360, (b) H-beta zeolite360-2wt%K, (c) H-beta zeolite360-4wt%K and (d) H-beta zeolite360-6wt%K 38

Figure 4. 3 The XRD pattern of H-beta zeolite and potassium modified H-beta zeolite 39

Figure 4. 4 The nitrogen adsorption-desorption isotherm of potassium modified 40

Figure 4. 5 The NH_3-TPD profile of H-beta zeolite and potassium modified H-beta zeolite catalysts. 42

Figure 4. 6 The CO_2-TPD profile of H-beta zeolite and potassium modified H-beta zeolite catalyst. 44

Figure 4. 7 The percent weight loss of potassium modified H-betazeolite360 catalysts after running reaction at reaction temperature 340 °C for 3 hr. 46

Figure 4. 8 The lactic acid conversion and products selectivity of H-beta zeolite and potassium modified H-beta zeolite catalysts at reaction temperature 340 °C and reaction time 120 minute. When AD, AA and PA are an acetaldehyde, acrylic acid and a propionic acid respectively. 48

Figure 4. 9 The lactic acid conversion of H-beta zeolite and potassium modified H-beta zeolite catalysts at temperature 340 °C 49

Figure 4. 10 The acrylic acid selectivity of H-beta zeolite and potassium modified H-beta zeolite catalysts at temperature 340 °C, (A), (B), (C) and (D) were potassium loading 0, 2, 4 and 6 wt% 49

Figure 4. 11 The acetaldehyde selectivity of H-beta zeolite and potassium modified H-beta zeolite catalysts at temperature 340 °C, (A), (B), (C) and (D) were potassium loading 0, 2, 4 and 6 wt% 50

Figure 4. 12 The propionic acid selectivity of H-beta zeolite and potassium modified H-beta zeolite catalysts at temperature 340 °C, (A), (B), (C) and (D) were potassium loading 0, 2, 4 and 6 wt% 50

Figure 4. 13 Potassium distribution on surface catalysts: (a) H-beta zeolite40-4wt%K, (b) H-beta zeolite360-4wt%K and (c) H-beta zeolite500-4wt%K 51

Figure 4. 14 The SEM images of all catalysts: (a) H-beta zeolite40-4wt%K, (b) H-beta zeolite360-4wt%K and (c) H-beta zeolite500 4wt%K 52

Figure 4. 15 The XRD pattern of modified H-beta zeolite catalysts with potassium loading 4 wt% 53

Figure 4. 16 The effect of potassium and temperature on framework structure of H-beta zeolite500 54

Figure 4. 17 The nitrogen adsorption-desorption isotherm of modified H-beta zeolite catalysts with potassium loading 4 wt%. 55

Figure 4. 18 The NH_3-TPD profile of modified H-beta zeolite catalysts with potassium loading 4 wt% 57

Figure 4. 19 The CO_2-TPD profile of modified H-beta zeolite catalysts with potassium loading 4 wt% 59

Figure 4. 20 The percent weight loss of loading potassium 4 wt% on H-beta zeolite catalyst with increase SiO_2/Al_2O_3 ratio 40, 360 and 500 after running reaction at reaction temperature 340 °C for 3 hr. 61

Figure 4. 21 The lactic acid conversion and products selectivity of loading 4wt%K on H-beta zeolite catalyst after run reaction temperature 340 °C and reaction time 120 minute. When AD, AA and PA are an acetaldehyde, acrylic acid and a propionic acid respectively. 63

Figure 4. 22 The lactic acid conversion of loading 4wt%K on H-beta zeolite catalysts after run reaction temperature 340 °C and reaction time 120 minute. 64

Figure 4. 23 The acrylic acid selectivity of loading 4wt%K on H-beta zeolite catalysts after run reaction temperature 340 °C, when (A), (B) and (C) were SiO_2/Al_2O_3 ratio 40, 360 and 500 respectively. 64

Figure 4. 24 The acetaldehyde selectivity of loading 4wt%K on H-beta zeolite catalysts after run reaction temperature 340 °C, when (A), (B) and (C) were SiO_2/Al_2O_3 ratio 40, 360 and 500 respectively. 65

Figure 4. 25 The propionic acid selectivity of loading 4wt%K on H-beta zeolite catalysts after run reaction temperature 340 °C, when (A), (B) and (C) were SiO_2/Al_2O_3 ratio 40, 360 and 500 respectively. 65

Figure B. 1 the calibration curve of ammonia from Micromeritics Chemisorp 2750 ... 75

Figure C. 1 the calibration curve of carbondioxide from Micromeritics Chemisorp 2750 76

Figure D. 1 The calibration curve of lactic acid..... 77

Figure D. 2 The calibration curve of acrylic acid..... 78

Figure D. 3 The calibration curve of acetaldehyde..... 78

Figure D. 4 The calibration curve of propionic acid..... 79

Figure D. 5 The calibration curve of 2,3-pentanedione..... 79

CHAPTER I
INTRODUCTION

1.1 Rationales

Presently, the interest of the raw material from biomass resource is increased due to the decrease of petroleum that affect to the rise of fossil raw material together with deterioration of environment [1]. Lactic acid is an important product that derived from biomass by fermentation technology of biomass material [2-5]. The lactic acid demand around the world in 2007 was estimated to 130,000-150,000 metric tons per year [6]. It contained two functional group are hydroxyl and carboxylic groups. So, it can be converted to other chemicals such as poly (lactic acid) (PLA), 2, 3-pentanedione (2, 3-PD), acetaldehyde (AD), propionic acid (PA) and acrylic acid (AA) [7-9]. Acrylic acid is an important raw material because it is used in a diverse range of applications including construction, automotive, packaging, health and personal care products such as diapers, detergents, surface coating, textile and inks [10]. However, the most of acrylic acid is derived from the oxidation reaction of propylene that is petroleum based. It is mixed with air and steam and reacted on a heterogeneous catalyst [11-14]. In order to solve these problems, the dehydration of lactic acid to acrylic acid is considered to be a sustainable alternative way due to lactic acid is derived from biomass.

The dehydration of lactic acid to acrylic acid is also accompanied with other competing reactions. The main of two side reaction are the decarboxylation of lactic acid to acetaldehyde that is more likely at a high acid amount catalyst while the condensation of lactic acid to 2, 3-pentanedione and reduction of lactic acid to propionic acid that is more likely at a low acid amount catalyst [15-17]. So, the suitable catalyst for dehydration of lactic acid to acrylic acid reaction should have balanced both acidity and basicity [7, 8].

The type of catalyst that mostly used to research for this reaction in gas phase condition is inorganic salt catalyst such as sulfates, nitrate and phosphate catalyst [18, 19]. However, sulfate and phosphate catalysts are used only at high temperature due

to the limit of amount surface active sites. Furthermore, the high temperature can be the cause of decarboxylation that is one of the key side reaction of lactic acid to acetaldehyde that effect to the decrease of the selectivity for acrylic acid. Furthermore, the deposition of coke that usually occurs at high temperature affect to deactivation of catalyst [16, 20].

Recently, the zeolite based catalysts are used extensively in industrial processes because their special properties such as high surface area, higher reaction temperatures due to the thermal stability of zeolites, shape-selectivity and high acid properties [21, 22]. However, the catalyst for this reaction don't need high acid properties. So, it is modified in order to decrease the acid properties before being used in the dehydration of lactic acid to acrylic acid [17, 21]. Alkali metals salt are often used to modify acid properties of ZSM-5 zeolite and NaY-zeolite catalyst for dehydration of lactic acid to acrylic acid. Due to the acid properties modification of zeolite, decarboxylation of lactic acid to acetaldehyde are inhibited and increase the selectivity of acrylic acid [17, 20]. The beta zeolite catalysts have been widely used in industries due to their easily adjust acid–base properties [23].

In this research, we modified H-beta zeolite with various SiO_2/Al_2O_3 ratios by potassium salt to adjust acid and base properties of catalyst for catalytic dehydration of lactic acid to acrylic acid and studied the effect of potassium to catalytic performance of catalyst.

1.2 Research objective

1.2.1 To study the effect of potassium on catalytic performance of H-beta zeolite for dehydration of lactic acid to acrylic acid.

1.2.2 To study the effect of SiO_2/Al_2O_3 ratios of H-beta zeolite on the catalytic performance of H-beta zeolite catalyst for dehydration of lactic acid to acrylic acid.

1.3 Research scope

1.3.1 The H-beta zeolite was modified with potassium nitrate by incipient wetness impregnation method with various SiO_2/Al_2O_3 ratios.

1.3.2 The catalysts were characterized by

- Scanning electron microscopy (SEM) and energy x-ray spectroscopy (EDX) for the morphology structure of catalysts.
- The X-ray diffraction (XRD) for crystalline phase of catalyst.
- The nitrogen physisorption for the specific surface areas, pore volume and pore diameter of catalysts.
- Ammonia temperature programed desorption (NH_3-TPD) for the acid properties of catalysts.
- Carbon dioxide temperature programed desorption (CO_2-TPD) for the base properties of catalysts.
- Thermal gravimetric and differential thermal analysis (TG-DTA) for the coke deposition of catalyst.

1.3.3 The investigation of catalytic performance of modified H-beta zeolite catalysts for dehydration of lactic acid to acrylic acid will be performed in these conditions

- Atmospheric pressure.
- Vaporizer temperature 230 °C
- Reaction temperature 340 °C
- 34% by volume lactic acid solution.
- 40 ml/min of gas flowrate balanced by nitrogen.

1.3.4 The compositions of reactants and products were analyzed by gas chromatograph equipped with DB-WAX UL column and flame ionization detector (FID).

1.4 Research and Methodology

1.4.1 Part I: The effect of potassium loading on catalytic activity

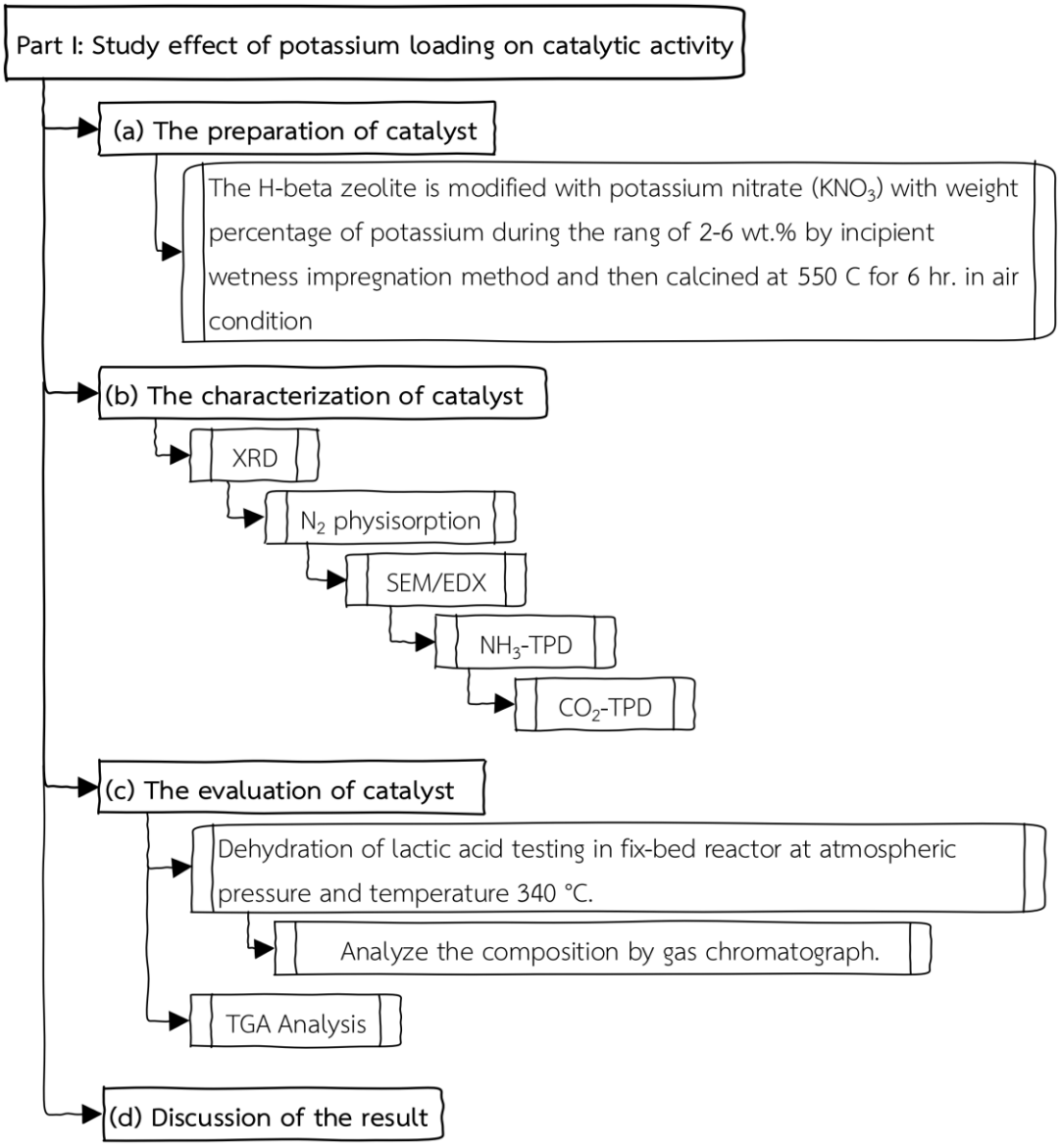

1.4.2 Part II: The effect of SiO_2/Al_2O_3 ratios of H-beta zeolite on catalytic activity

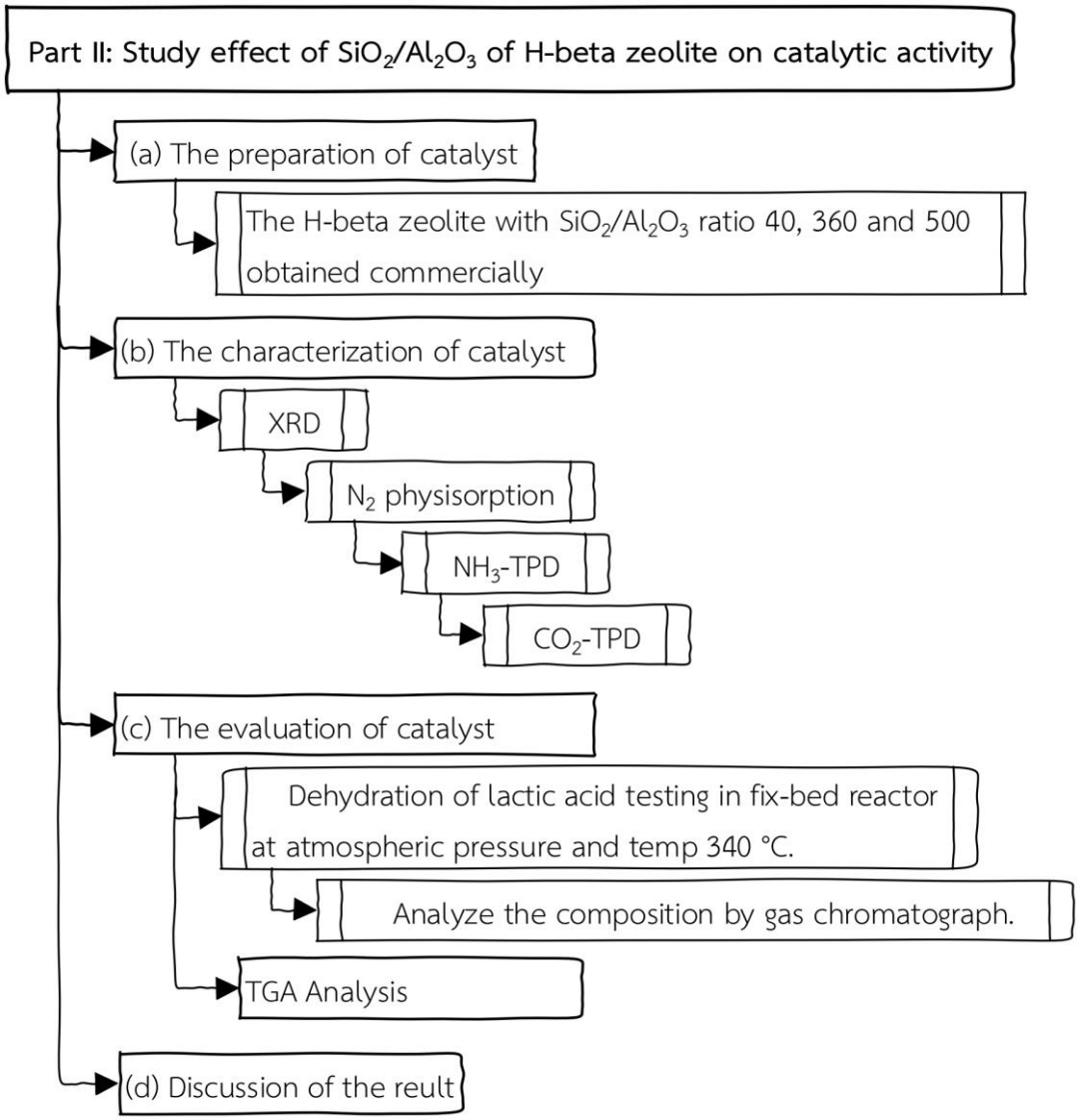

CHAPTER II
THEORY AND LITERATURE REVIEW

2.1 Reactant and Product

2.1.1 Lactic acid

Lactic acid or 2-hydroxypropanoic acid is an organic acid widely used in industrial. The worldwide demand of lactic acid in 2007 was estimated to be 130,000 to 150,000 metric tons per year. The mostly of lactic acid is derived by fermentation method of biomass material such as starch, cassava powder, sugarcane juice, glucose etc. Lactic acid have two form are L (+) lactic acid and D (-) lactic acid isomer [6].

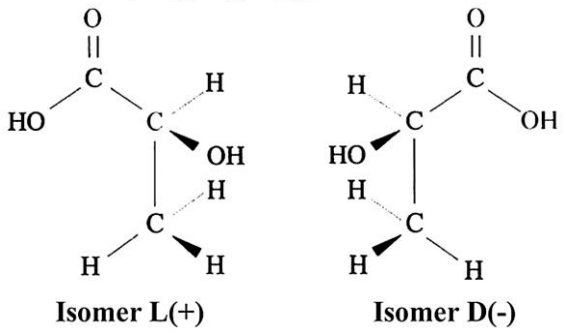

Figure 2. 1 Structure of L (+) and D (-) isomers of the lactic acid [24].

The chemical and physical properties of lactic acid is shown that in Table 2.1

Table 2. 1 The chemical and physical properties of lactic acid [7].

Properties	Unit or Condition	Isomer	Reported Rang
Melting point	°C	L or D	52.7-53.0
Boiling point	°C (at 1.87 kPa)	L or D	103
Solid density	g/mL (at 20 °C)	-	1.33
Liquid density of aq. solution	g/mL (at 25 °C)	L or D	1.057
pK_a		L or D	3.79-3.86

The functional group of lactic acid contain hydroxyl and carboxylic groups that can be converted to other chemicals such as acetaldehyde (AD), acrylic acid (AA), poly(lactic acid) (PLA), 2, 3-pentanedione (2,3-PD) and propionic acid (PA) [7-9].

2.1.2 Acrylic acid

Acrylic acid is an important raw material because it is used in a diverse range of applications including construction, automotive, packaging, health and personal care products such as diapers, detergents, surface coating, textile and inks [10]. The most of acrylic acid is derived from the oxidation reaction of propylene that is petroleum based. It is mixed with air and steam and reacted on a heterogeneous catalyst.

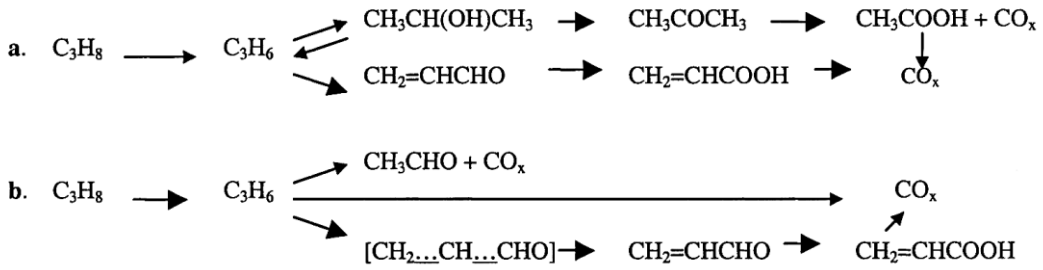

Figure 2. 2 Oxidation reaction pathway of propylene to acrylic acid (a) Te/VPO and (b) Te–P/NiMoO catalysts [25].

Table 2. 2 The chemical and physical properties of acrylic acid.

Chemical formula	$C_3H_4O_2$
Molar mass	72.06 g/mole
Appearance	clear, colorless liquid
Odor	Acrid
Density	1.051 g/mL
Melting point	14 °C (57 °F; 287 K)
Boiling point	141 °C (286 °F; 414 K)
Solubility in water	Miscible
Acidity (pKa)	4.25

2.2 Dehydration reaction of lactic acid to acrylic acid

2.2.1 Side reaction in the dehydration reaction of lactic acid

The dehydration of lactic acid to acrylic acid is accompanied with other product that shown figure 2.3

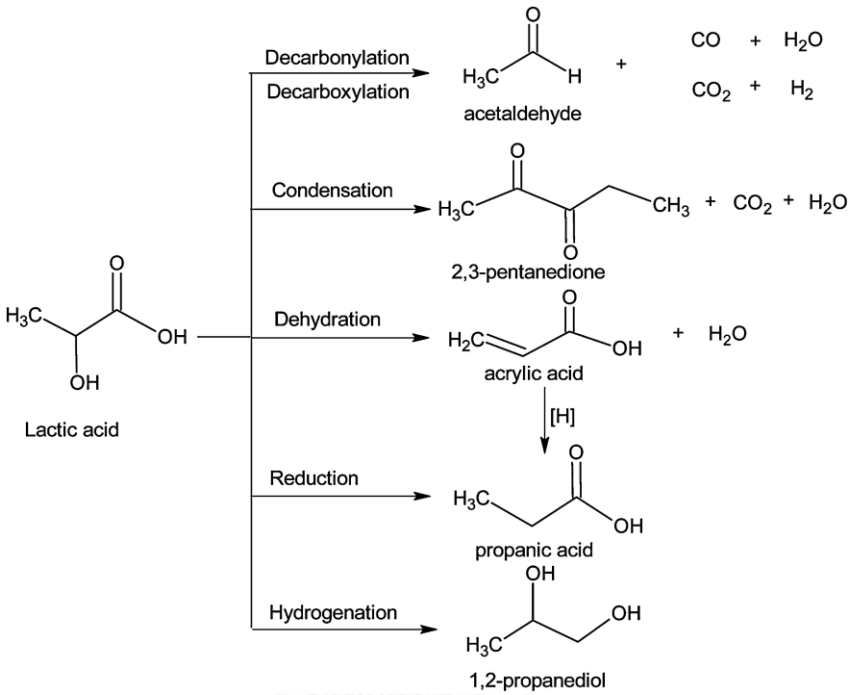

Figure 2. 3 Main conversion pathways of lactic acid in the gas phase reaction [15].

The main side product in the dehydration of lactic acid to acrylic acid are acetaldehyde, 2, 3-pentanedione and propionic acid. The acetaldehyde is derived from decarbonylation reaction that is activated by Brønsted acid site in catalyst on the carboxylic group of the lactic acid molecule and decarboxylation reaction that is enabled by the nucleophilic activation of the carboxylic group of the lactic acid molecule. While, the 2, 3-pentanedione and propionic acid is by-product over basic catalyst and at high pressure [26].

2.2.2 The mechanism on heterogeneous catalyst

The mechanism of lactic acid dehydration reaction on heterogeneous catalyst start with the attraction of **α**-hydroxyl group in molecule of lactic acid by acid site on surface catalyst and an attack on **β**-hydrogen by basic site to form cyclic transition state with the C2 and C3 atoms of the lactic acid molecule and then loss of the **α**-hydroxyl group and **β**-hydrogen via E2 elimination mechanism [27].

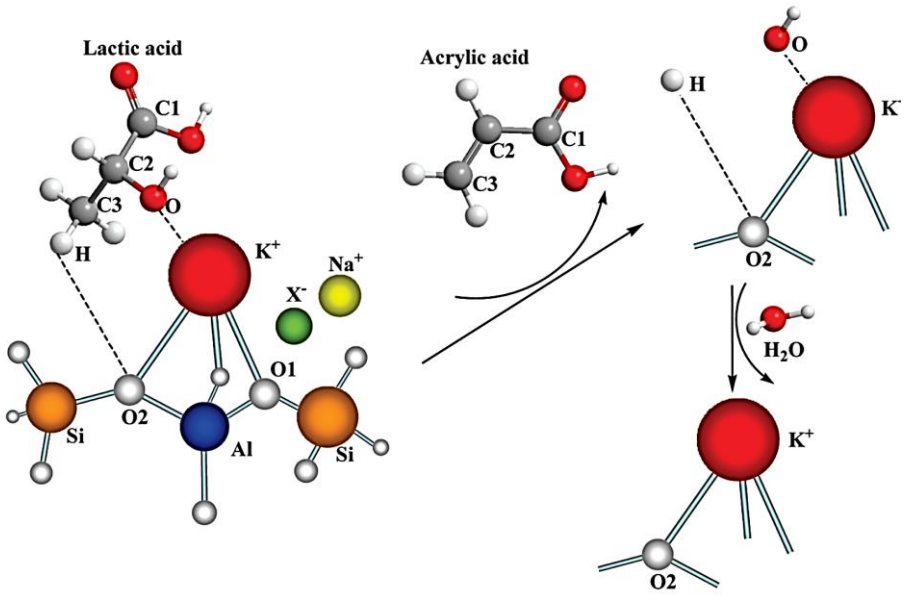

Figure 2. 4 The mechanism of lactic acid dehydration to acrylic acid reaction on modified NaY-zeolite catalyst [27].

2.2.3 The kinetic of lactic acid dehydration

A kinetic model (Table 2.3) which predicts the favorability of acrylic acid formation at high temperatures, short contact times and low pressures over sodium nitrate on silica catalyst.

Table 2. 3 the kinetic data of lactic acid dehydration [9].

Reaction		Reaction order	Preexponential factor ($k_{i,0}$)	Activation energy (kJ/mole)
Lactic acid ⟶	Acetaldehyde	1	9.7×10^{9} s^{-1}	115
Lactic acid ⟶	2,3-pentanedione	2	6.5×10^{10} s^{-1}	110
Lactic acid ⟶	Acrylic acid	1	1.9×10^{11} s^{-1}	137

2.3 Zeolite catalyst

2.3.1 Structures and definitions

Zeolites are aluminosilicates crystalline of aluminate (AlO_4) and silicate (SiO_4) tetrahedral that linked through oxygen atoms. These result is macromolecule with a structurally distinct three dimensional framework that containing channels and cavities of molecular with dimensions [22, 28]. The general formula representing their structure could be written as follows:

$$A^{m+}_{y/m}[(SiO_2)_x \cdot (AlO^-_2)_y] \cdot zH_2O$$

From the general formula, A is a cation with the charge +m which balances the positive charge due to negative charge of (AlO^-_2) groups. The sum of x+y is the number of tetrahedral in a unit cell of the particular zeolite and the ratio x/y is the Si to Al ratio which is importance parameter for zeolite's properties [28].

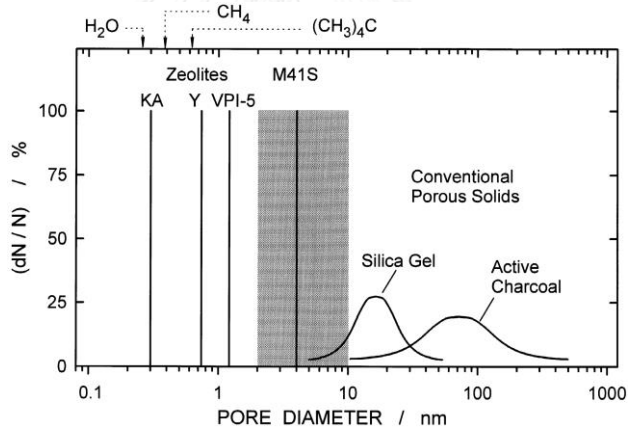

Figure 2. 5 Typical pore diameter distributions of porous solids [28].

The zeolite was used extensively in applications including ion exchangers, adsorbents and catalysts such as cracking, hydrocracking and isomerization due to their characteristic properties being high sure area, high reaction temperature due to the thermal stability of zeolites, easy regeneration of the catalyst upon thermal treatment and molecular dimensions of the pores. When compared the unique features between zeolite and solid catalysts or catalyst supports result that their strictly uniform pore diameters and pore widths in the order of molecular dimensions and zeolites are typical microporous materials [29, 30].

2.3.2 Beta zeolites catalysts

Beta zeolite (BEA) has been known since 1967 and showed high catalytic activity. Its crystalline structure has been determined and shown that its void structure is available. It has a total pore volume of around 0.2 ml/g. It is proposed that the pore structure consists of channels of 12-membered rings interconnected by cages constituted by the intersections of the channels.

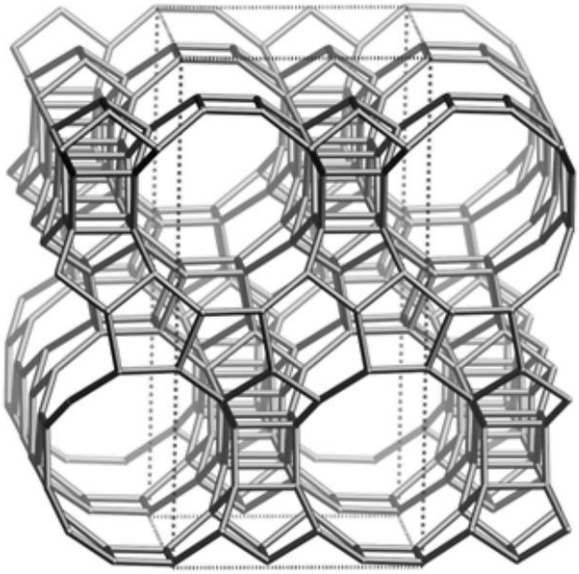

Figure 2. 6 Structure of H-beta zeolite [31].

Beta zeolite has a substantial industrial importance. It has been successfully used for acid catalyzed reactions in the petrochemical industry such as catalytic cracking, aromatic and aliphatic alkylation because of its properties are high surface area, high thermal stability and high acidity peculiar system [32, 33]. Moreover, it can be easily adjustable acid–base properties [34].

2.4 Deactivation of catalyst

Catalyst deactivation is the one of major problem of heterogeneous catalyst because of it is a reason of decrease catalytic performance such as catalytic activity or selectivity of catalyst. The commonly classes of deactivation are poisoning, sintering, coking and fouling [35, 36].

2.4.1 Poisoning

Poisoning is the strong chemisorption of reactants, products or impurities on active sites of catalyst. So it cause of the restructuring of the surface by the strongly adsorbed poison, possibly causing dramatic changes in catalytic properties, the adsorbed poison blocks access of adsorbed reactants to each other and finally prevents or slows the surface diffusion of adsorbed reactants [36].

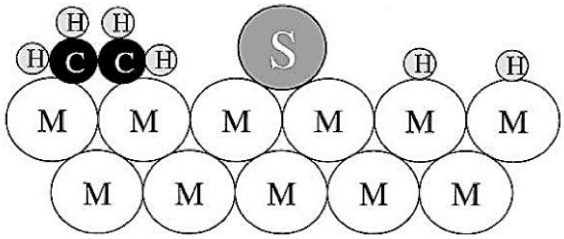

Figure 2. 7 The poisoning model during ethylene hydrogenation by sulfur atom at metal surface [36].

2.4.2 Sintering

Sintering is the loss of catalytic surface area due to crystallite growth of the catalytic phase or loss of support area due to support collapse that often involved with thermally. Sintering processes generally occurred at high reaction temperatures (e.g. >500°C) [35, 36].

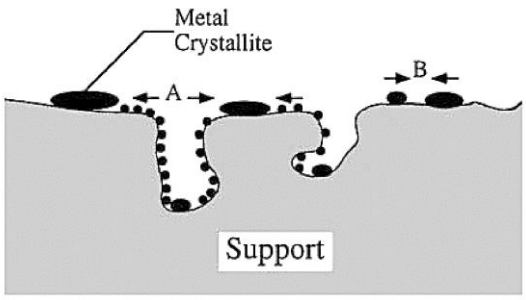

Figure 2. 8 Two sintering model due to growth of crystallite (A) atomic migration or (B) crystallite migration [36].

2.4.3 Fouling

Fouling is the deactivation that occurred from physical deposition of carbon species onto surface catalyst such as deposits of carbon and coke in porous catalysts. As a result, the activity of catalyst are loss due to the active site on surface catalysts are blockaded. Coking is derived by decomposition or condensation of hydrocarbons on surface catalyst and consists of polymerized heavy hydrocarbons that its chemical structure are varied with type of reaction, catalyst and conditions [35, 36].

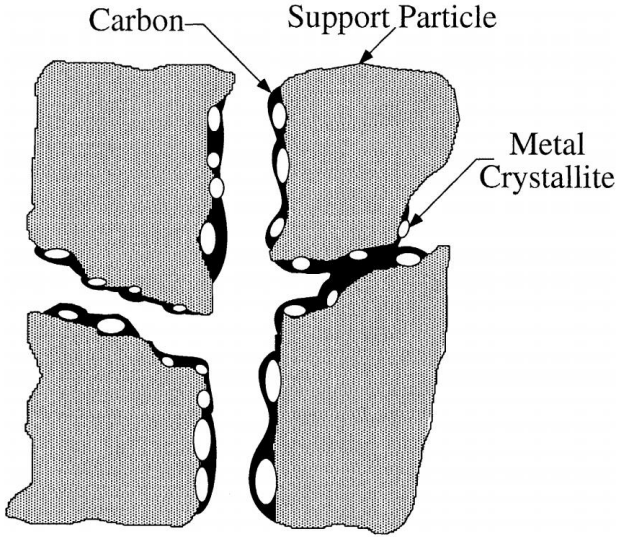

Figure 2. 9 The fouling model of a supported metal catalyst due to carbon deposition [36].

2.5 Literature review

The dehydration reaction of lactic acid to acrylic acid is also accompanied with other products. The two main side products are acetaldehyde and 2, 3-pentanedione whereas acetaldehyde is derived from the decarboxylation and decarbonylation while 2, 3-pentanedioneis derived from the condensation of lactic acid. To inhibit the formation of acetaldehyde and 2, 3-pentanedioneis and improve the selectivity of acrylic acid, various kinds of catalyst have been widely studied.

2.5.1 Suitable properties of catalyst for dehydration of lactic acid to acrylic acid.

Various types of catalyst were used to research for lactic acid dehydration reaction such as sulphates [37], pyrophosphate [38], hydroxyapatite [39] and zeolite catalysts including NaY zeolite [27, 40, 41], ZSM-5 zeolite [16, 20] and Beta zeolite [42, 43].

For the test of catalysts, sulphate catalysts that modified with various metals (Ni, Zn, Mg, Ba, Ca and Na), resulting in the increase of medium acidity strength, can increase selectivity of acrylic acid. The $BaSO_4$ catalyst exhibited highest catalyst performances with 99.8% lactic acid conversion and 74.0% acrylic acid selectivity at reaction temperature of 400 ^{o}C [37]. Meanwhile, pyrophosphate catalyst modified with strontium metal demonstrated that the catalytic activity of catalyst depends on the surface acidity. Strontium pyrophosphate catalyst exhibited 100% lactic acid conversion and 72.2% acrylic acid selectivity at reaction temperature of 400 ^{o}C due to a medium acidity [38]. It has been concern that the high reaction temperature can cause the carbon deposition and decrease stability of carboxylic acid group of lactic acid affecting to promote decarbonylation and decarboxylation reaction [20, 26]. The hydroxyapatite catalyst with various Ca/P ratios can be used for this reaction at temperature of 360 ^{o}C which was lower than the reaction temperature of sulphates and pyrophosphate catalysts. In addition, the catalytic activity relates with the acidity/basicity ratio on catalyst surface. The hydroxyapatite catalyst exhibited high acrylic acid selectivity of 71%, however only 70% lactic acid conversion was obtained [39].

Many types of zeolite were improved their acidity and basicity properties before being used in this reaction. The modification of zeolite mostly used alkaline and alkali-earth metal by impregnation and ion-exchange method such as NaY zeolite modified with potassium salt [27], Na_2HPO_4/NaY zeolite [41], NaY zeolite modified with alkali-earth metal [21], ZSM-5 and Beta zeolite modified alkaline metal [16, 20, 42, 43]. Especially, potassium (K) can improve the acid and base properties of zeolites affecting to the inhibition of acetaldehyde formation from decarbonylation and decarboxylation reaction and the promotion of the acrylic acid formation from lactic acid dehydration reaction [16, 27]. For instance, the KI/NaY zeolite catalyst prepared via impregnation method showed 97.6% lactic acid conversion and 67.9% acrylic acid selectivity at reaction temperature of 325 ^{o}C [27], the K/ZSM-5 zeolite catalyst that prepared via ion-exchange method show 95.21% lactic acid conversion and 76.47% acrylic acid selectivity at reaction temperature 365 ^{o}C [20]. However, not only does the acrylic acid selectivity depend on acid and base properties of catalyst, but also on integrity of crystallinity structure of catalyst [16].

The treatment of zeolite catalyst with alkaline solution affects the crystallinity structural collapse of zeolite due to the removal of Si atom or desilication. The degree of crystallinity structural collapse of zeolite corresponds to FER > MOR > MFI >BEA zeolite [44].

From the studies of all the above literature review, it has been found that the suitable catalyst for the dehydration of lactic acid to acrylic acid reaction should have good balance of both acidity and basicity as well as the integrity of catalyst structure. The beta zeolite catalyst seems to be suitable to be used for lactic acid dehydration reaction combined with improved acidity and basicity properties made via potassium metal modification.

2.5.2 Suitable reaction condition for dehydration of lactic acid to acrylic acid.

When the reaction temperature was increased from 330 °C to 400 °C, the conversion of lactic acid also increased as the lactic acid dehydration reaction is an endothermic reaction. On the other hand, the acrylic acid selectivity was maximized during the range of reaction temperatures of 330 °C to 370 °C, depending on type of catalyst and other conditions [15, 16, 20]. Neither an excessively lower nor, higher temperature is profitable to the formation of acrylic acid as the temperature lower than 300 °C is beneficial to the formation of 2,3-pentandione [45]. At high temperature, the stability of carboxylic acid group of lactic acid decreased, which favorably affected decarboxylation and decarbonylation reaction to form acetaldehyde as byproduct [26].

CHAPTER III

EXPERIMENTAL

This chapter involved the research experiments consisted of three section. First section was preparation of catalyst prepared by incipient wetness impregnation method. Second section was characterization of catalyst by X-Ray Diffraction (XRD) Nitrogen physisorption Scanning electron microscopy (SEM) and energy x-ray spectroscopy (EDX) Ammonium temperature programed desorption (NH_3-TPD) Carbon dioxide temperature programed desorption (CO_2-TPD) and Thermal gravimetric and differential thermal analysis (TG-DTA). The final section was dehydration of lactic acid testing.

3.1 Preparation of catalyst

3.1.1 Chemicals

- H-beta zeolite obtained commercially with SiO_2/Al_2O_3 ratios of 40, 360 and 500.
- Potassium nitrate (KNO_3)
- Deionized water.

3.1.2 The incipient wetness impregnation method preparation of catalysts.

Firstly, the purchased H-beta zeolites were dried to completely remove moisture. Next, prepared KNO_3 aqueous solution by dissolving KNO_3 in a deionized water with desired weight percentage of KNO_3. Then drop the solution of KNO_3 onto H-beta zeolite that was calcined with volume of solution equal pore volume of H-beta zeolite. The mixture was kept at room temperature for 5 h in hood. Finally, the catalysts were dried at 110 ℃ overnight and calcined at 550 ℃ in air for 6 h to obtain the modified H-beta zeolite catalysts (H-beta zeolite-x-y) where x and y represent the SiO_2/Al_2O_3 ratio of H-beta zeolites and the weight percentage of potassium in H-beta zeolite, respectively.

3.2 Characterization of Catalyst

3.2.1 X-Ray Diffraction (XRD).

X-ray diffraction (XRD) patterns of powder catalysts were measured by the SIEMENS D5000 X-ray diffractometer with a Cu K_{α} radiation source. The XRD patterns were collected with the 2θ in range of 10-60 degree with rate of 2.5 degree/min.

3.2.2 Nitrogen physisorption (BET)

The specific surface areas, pore volume and pore diameter of catalysts were determined by nitrogen gas adsorption-desorption technique at liquid nitrogen temperature (-196 ºC) with Micromeritics Chemisorb 2750 Pulse Chemisorption System instrument. The specific surface area was calculated form the Brunauer-Emmett-Teller (BET), while pore volume was evaluated from the t-plot method.

3.2.3 Scanning electron microscopy (SEM) and energy x-ray spectroscopy (EDX)

The morphology and elemental dispersion over the catalysts surface were determined by scanning electron microscope (SEM) and energy X-ray spectroscopy (EDX), respectively. The SEM model is JEOL mode JSM-5800LV and Link Isis Series 300 program was performed for EDX.

3.2.4 Ammonium temperature programed desorption (NH_3-TPD)

The acid properties of catalysts were investigated by Ammonium temperature programed desorption (NH_3-TPD) technique by using Micromeritics Chemisorb 2750 Pulse Chemisorption System.

3.2.5 Carbon dioxide temperature programed desorption (CO_2-TPD).

The base properties of catalysts were investigated by carbon dioxide temperature programed desorption (CO_2-TPD) technique by using Micromeritics Chemisorb 2750 Pulse Chemisorption System.

3.2.6 Thermal gravimetric and differential thermal analysis (TG-DTA).

The coke deposition of catalyst was investigated by thermal gravimetric analysis (TGA) and differential thermal analysis (DTA) technique under the temperature range of 20-1000 ºC with a heating rate of 10 ºC /min in oxygen atmosphere.

3.3 Dehydration of Lactic Acid Testing.

3.3.1 Chemicals and Reactant.

- Lactic Acid Solution
- Nitrogen Gas.

3.3.2 Instrument and Apparatus.

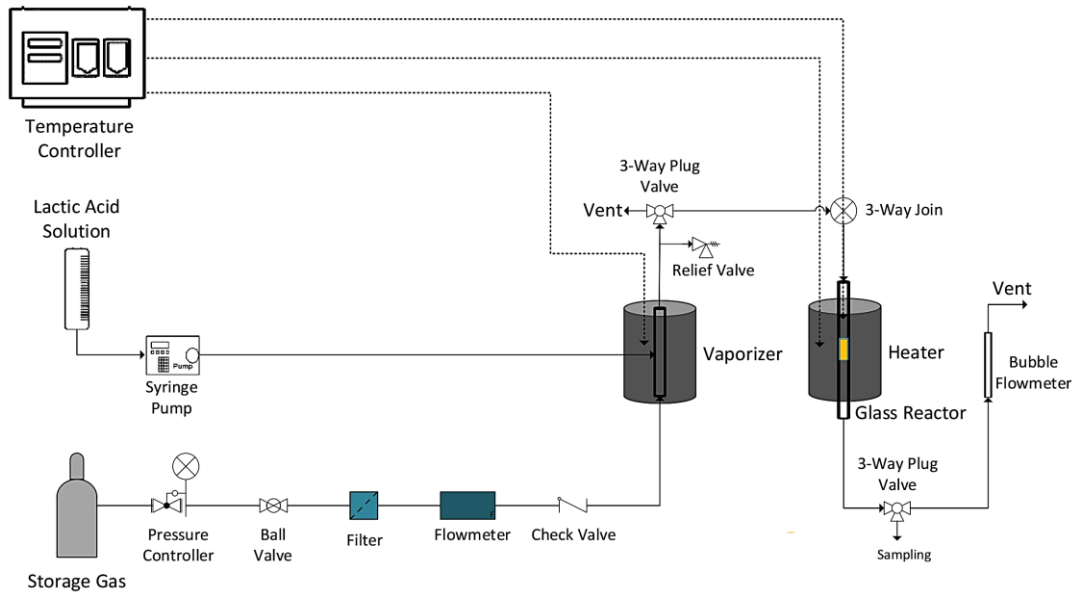

Figure 3. 1 Experimental set-up for reaction test.

- **Syringe pump:** The syringe pump is used to inject lactic acid solution into the vaporizer.
- **Vaporizer:** The vaporizer is an equipment to vaporize lactic acid solution from liquid phase to vapor phase. It is operated at atmospheric pressure with temperature 230 ºC that it is higher than the boiling point of lactic acid of 218 ºC. So, the lactic acid can be vaporized to vapor phase.
- **Storage Gas:** The nitrogen gas is a carrier gas for used to carry vapor of lactic acid into the reactor
- **Glass Reactor:** The glass reactor is filled with catalyst for fixed-bed reactor where the reaction takes place. It is made of glass tube with an inside diameter of 9 mm.

- **Heater:** The heater is used to heat the fixed-bed reactor tube. The temperature of the fixed-bed reactor is controlled by temperature controller.
- **Temperature controller:** The temperature controller is an equipment that used to control the temperature of the vaporizer and reactor. For the vaporizer, the temperature is controlled at 230 ºC, for the fixed-bed reactor, the temperature is controlled at 340 ºC.
- **Sampling:** The sample is collected at product sampling points to be analyzed by gas chromatograph.
- **Gas chromatography (GC):** The gas chromatograph is used to investigate conversion and selectivity of product. It is equipped with DB-WAX UL column and flame ionization detector (FID).

Table 3. 1 Operating conditions of gas chromatographs

Gas Chromatograph	**Shimudzu, GC14-B**
Detector	FID
Column	DB-WAX capillary
Carrier gas	Nitrogen
Initial column temperature	230
Final column temperature	230
Detector temperature	230
Injector temperature	230
Time analyzed	10 min.

3.3.3 Dehydration Reaction of Lactic Acid Procedure.

The dehydration reaction of lactic acid was carried out with continuous flow in vertical fixed-bed reactor with inner diameter 9 mm and operated under atmospheric pressure. In the experiment, 0.1 g of a packed quartz wool and 0.02 g of catalyst was loaded into the reactor and then the reactor was packed in the center of a furnace and heated. The firstly, the catalyst was preheated at the reaction temperature for 1 hour with nitrogen gas flow rate 40 mL/min under atmospheric pressure. Then, the lactic acid solution was injected by syringe pump into the vaporizer and driven to reactor by nitrogen gas with flow rate 40 mL/min. The reaction temperature was fixed at 340 °C in each run. Finally, The product (gas phase) was injected into the gas chromatograph with FID using DB-WAX UL column

CHAPTER IV
RESULTS AND DICCUSSION

This chapter involved the results and discussion of research that consisted of two section. First section explained the effect of potassium loading of potassium nitrate (KNO_3) on catalytic performance of H-beta zeolite catalyst for dehydration of lactic acid to acrylic acid reaction via incipient wetness impregnation method. The final section explained the effect of SiO_2/Al_2O_3 ratios of H-beta zeolite modified with potassium nitrate (KNO_3) on catalytic performance for dehydration of lactic acid to acrylic acid reaction.

4.1 The effect of potassium loading on catalytic activity

4.1.1 Characterization of Catalyst

4.1.1.1 Scanning electron microscopy (SEM) and energy x-ray spectroscopy (EDX)

The morphology and elemental composition over the catalysts surface were determined by scanning electron microscope (SEM) and energy X-ray spectroscopy (EDX), respectively. The SEM model is JEOL mode JSM-5800LV and Link Isis Series 300 program was performed for EDX.

Table 4. 1 The element composition of catalyst from energy X-ray spectroscopy

Catalysts	Weight%			
	O	Al	Si	K
H-beta Zeolite360-0wt%K	49.00	1.02	49.98	0.00
H-beta Zeolite360-2wt%K	47.54	1.02	48.42	3.02
H-beta Zeolite360-4wt%K	49.36	0.95	45.44	4.25
H-beta Zeolite360-6wt%K	46.72	1.43	45.51	6.34

The element composition of all catalysts is shown in Table 4.1, the value of potassium composition analyzed by energy X-ray spectroscopy (EDX) was more than that calculated in every sample. The potassium composition from energy X-ray spectroscopy (EDX) is potassium composition at surface catalyst only.

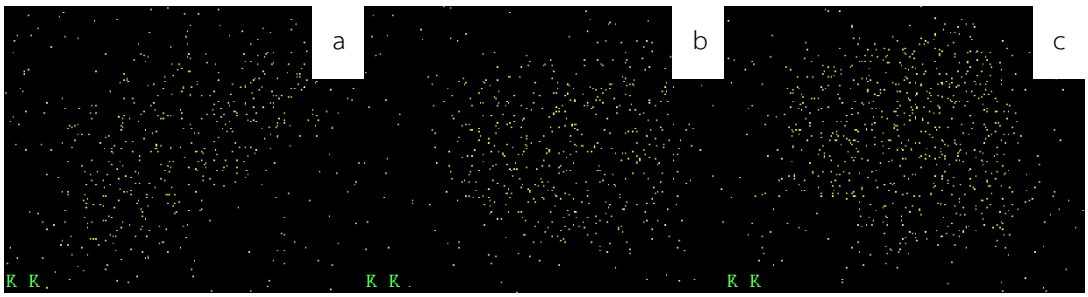

Figure 4. 1 Potassium distribution on surface of modified H-beta zeolite360 catalysts: (a) Potassium 2wt%K, (b) Potassium 4wt%K and (c) Potassium 6wt%K

The potassium distribution on surface of H-beta zeolite360 is shown in Fig. 4.1 indicating that potassium can be dispersed on surface of H-beta zeolite360 catalyst. The scanning electron microscopy of H-beta zeolite360 and potassium modified H-beta zeolite360 shown in Fig. 4.2 indicating that the morphology of crystalline has spherical shape and the size of particle distribution is a narrow distribution.

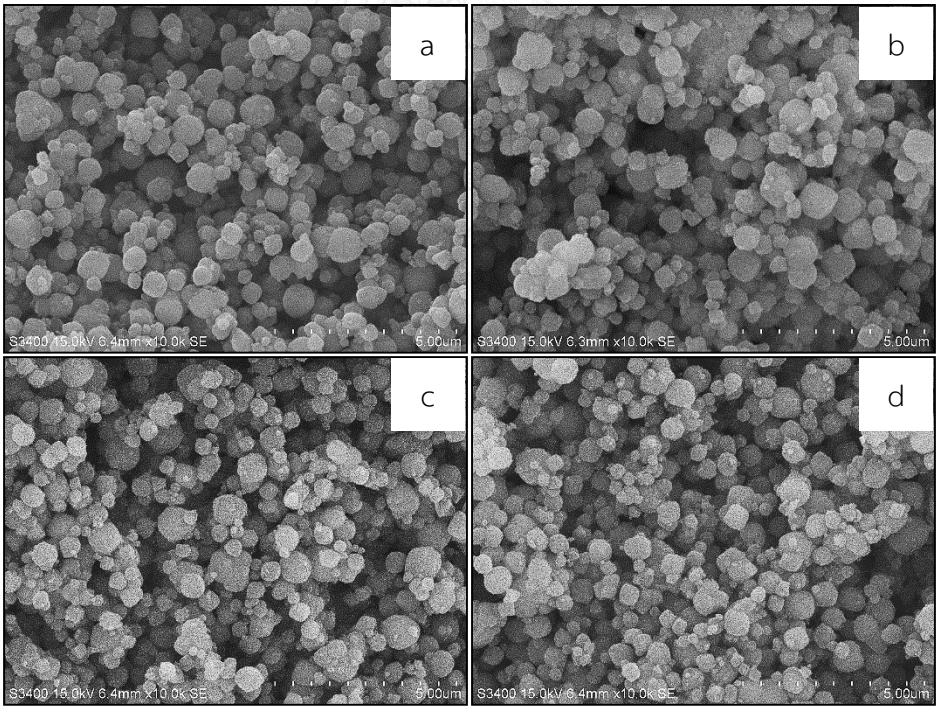

Figure 4. 2 SEM images of the H-beta zeolite360 and the modified H-beta zeolite360 catalysts: (a) H-beta zeolite360, (b) H-beta zeolite360-2wt%K, (c) H-beta zeolite360-4wt%K and (d) H-beta zeolite360-6wt%K

4.1.1.2 X-Ray Diffraction (XRD).

The X-ray diffraction (XRD) patterns of H-beta zeolite360 and potassium modified H-beta zeolite360 catalysts were measured by the SIEMENS D5000 X-ray diffractometer with a Cu K_α radiation source. The XRD patterns were collected with the 2θ in range of 10 to 70 degree with rate of 2.5 degree/min.

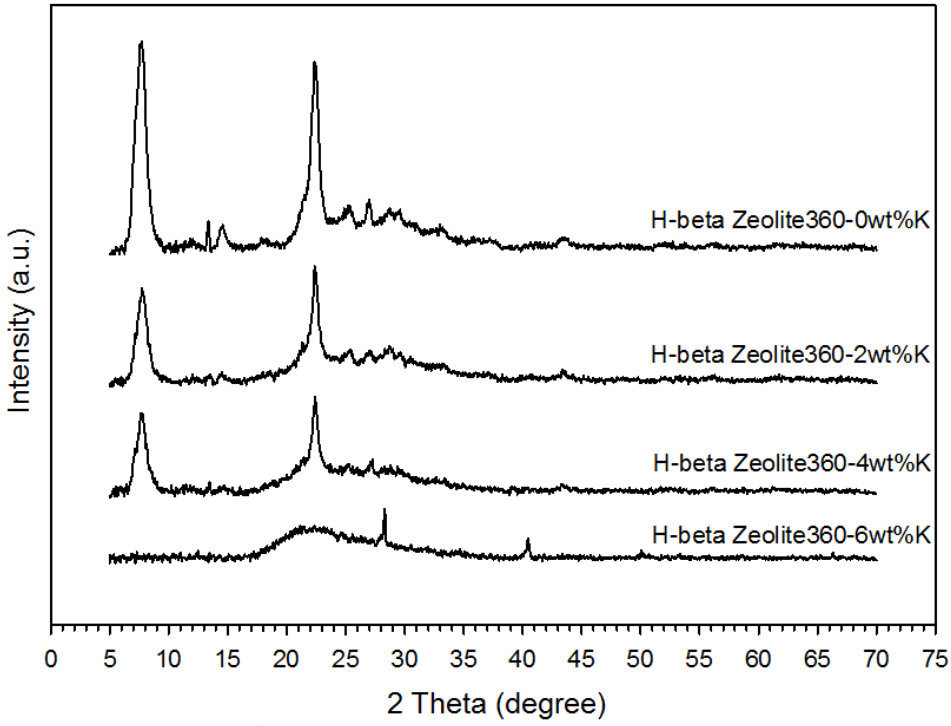

Figure 4. 3 The XRD pattern of H-beta zeolite and potassium modified H-beta zeolite

The XRD patterns of H-beta zeolite360 and potassium modified H-beta zeolite360 are shown in Fig. 4.3. The characteristic peaks of H-beta zeolite catalyst within the 2θ range of 5-70 degree were 7.8, 16.5, 22.5, 25.3, 26.9, 29.5 and 43.5 degree [46]. As shown in Fig. 4.3, all of the potassium modified H-beta zeolite catalyst except H-beta zeolite360-6wt%K retain the characteristic peak of H-beta zeolite indicating that they retain the basic structure of H-beta zeolite catalyst after loaded with potassium. On the other hand the intensities of these peaks decrease with the increasing potassium loading, indicating that potassium loading resulted in the crystallinity structural collapse of H-beta zeolite catalysts [46].

4.1.1.3 Nitrogen physisorption

The nitrogen adsorption-desorption isotherm of H-beta zeolite360 and potassium modified H-beta zeolite360 catalysts are shown in Fig. 4.4. The surface area of catalysts was measured by N_2-physisorption and the results are shown in Table 4.2.

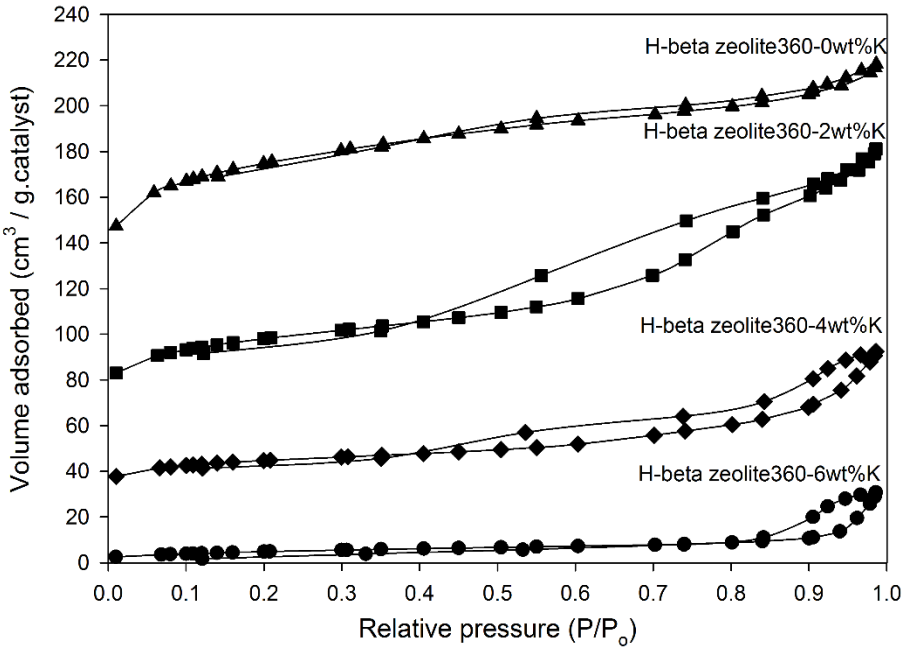

Figure 4. 4 The nitrogen adsorption-desorption isotherm of potassium modified H-beta zeolite catalysts.

Table 4. 2 The physical properties of potassium modified H-beta zeolite catalysts.

Catalysts	Surface area* (m^2/g)	Micropore volume** (cm^3/g)	Average pore size*** (nm)
H-beta zeolite360	595	0.192	2.5
H-beta zeolite360-2wt%K	333	0.103	3.3
H-beta zeolite360-4wt%K	152	0.047	3.7
H-beta zeolite360-6wt%K	11	0.002	10.2

*The surface area was calculated by Brunauer–Emmett–Teller (BET) method.

**The micropore volume was evaluated by t-plot method.

***The average pore size was evaluated by adsorption average pore width (4V/A BET).

As shown in Fig. 4.4, all of catalysts conformed to the nitrogen adsorption-desorption isotherm type IV. The Hysteresis loop indicating that multiple rang of physisorption isotherm that corresponding to the filling and emptying of mesopore of surface catalysts with pore size during the range of 2 to 50 nm.

The surface area of catalysts were measured by N_2-physisorption and the results are shown in Table 4.2. the surface area and micropore volume of H-beta zeolite360 catalyst and potassium modified H-beta zeolite360 catalysts decreased from 595 to 11 m^2/g and from 0.192 to 0.002 cm^3/g respectively with the increasing potassium loading due to pore of catalyst was filled by potassium oxide. On the other hand, the average pore size of catalysts increased from 2.5 to 10.2 nm because of potassium loading that resulted in the crystallinity structural collapse of H-beta zeolite catalysts that discusses above.

4.1.1.4 Ammonia temperature-programed desorption (NH_3-TPD)

The acidity properties of surface catalyst was widely characterized by ammonia temperature program (NH_3-TPD). The NH_3-TPD profile of H-beta zeolite catalyst and potassium modified H-beta zeolite catalyst are shown in Fig. 4.5

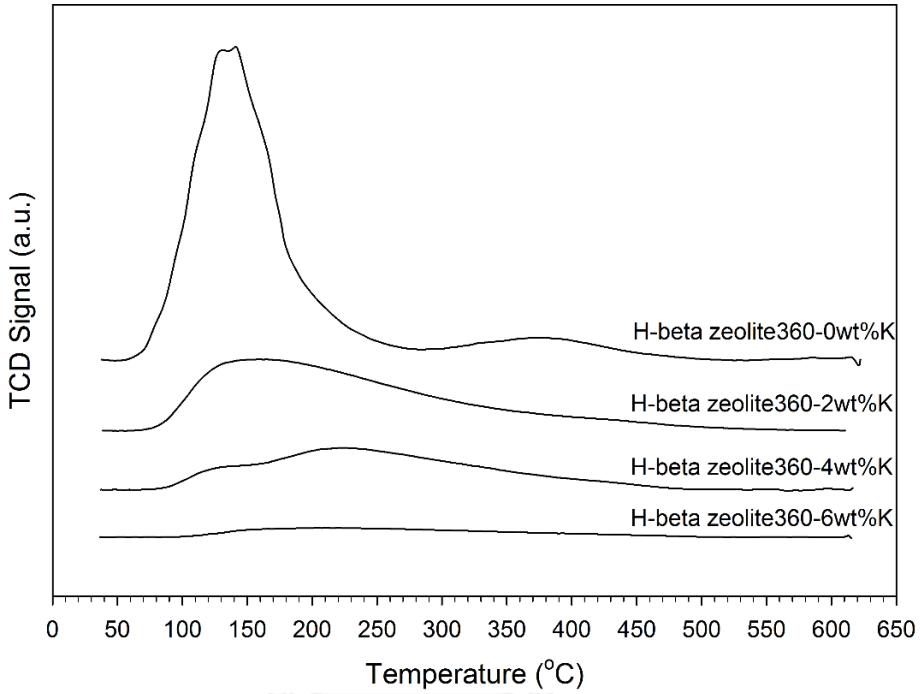

Figure 4. 5 The NH_3-TPD profile of H-beta zeolite and potassium modified H-beta zeolite catalysts.

Table 4. 3 The acidity properties of H-beta zeolite catalyst and potassium modified H-beta zeolite catalyst

Catalysts	Acid strength		Total acid
	weak	medium & strong	(mmol NH_3/g cat.)
H-beta Zeolite360	0.084	0.019	0.103
H-beta Zeolite360-2wt%K	0.040	0.010	0.050
H-beta Zeolite360-4wt%K	0.023	0.010	0.033
H-beta Zeolite360-6wt%K	0.006	0.002	0.008

The acid strength of catalyst related with the desorption temperature of ammonia [47]. Furthermore, the amount of total acidity related with the total amount ammonia desorption [48]. The desorption of ammonia during the temperature range lower than 250 ^{o}C was ascribed to weak acidity site, while these of temperature range upper than 250 ^{o}C were ascribed to medium and strong acidity site on surface catalyst [49]. As shown in Fig. 4.5, the area of peak at 140 ^{o}C decreased with the increasing potassium loading, indicating that the weak acidic site on surface catalysts was decreased when increase potassium loading. Furthermore, at peak 360 ^{o}C that corresponding to medium-strong acidic site property on surface of catalyst disappear when increase potassium loading. These result, indicates that the potassium addition of H-beta zeolite could not only decrease the acidity properties of H-beta zeolite, but also transforms the acid strength from medium-strong acid site to weak acid site. The acid properties of the catalysts were also summarized in Table 4.3

4.1.1.5 Carbondioxide temperature-programed desorption (CO_2-TPD)

The basicity properties of surface catalysts were characterized by carbondioxide temperature program (CO_2-TPD). The amount of total basicity related with the total amount carbondioxide desorption. The CO_2-TPD profile of H-beta zeolite catalyst and potassium modified H-beta zeolite catalyst are shown in Fig. 4.6, while the data of TPD of desorbed CO_2 is shown in Table 4.4

Table 4. 4 The basicity properties of H-beta zeolite catalyst and potassium modified H-beta zeolite catalyst

Catalysts	Total Base (umol CO_2/g cat.)
H-beta Zeolite360	0.000
H-beta Zeolite360-2wt%K	4.213
H-beta Zeolite360-4wt%K	15.950
H-beta Zeolite360-6wt%K	1.840

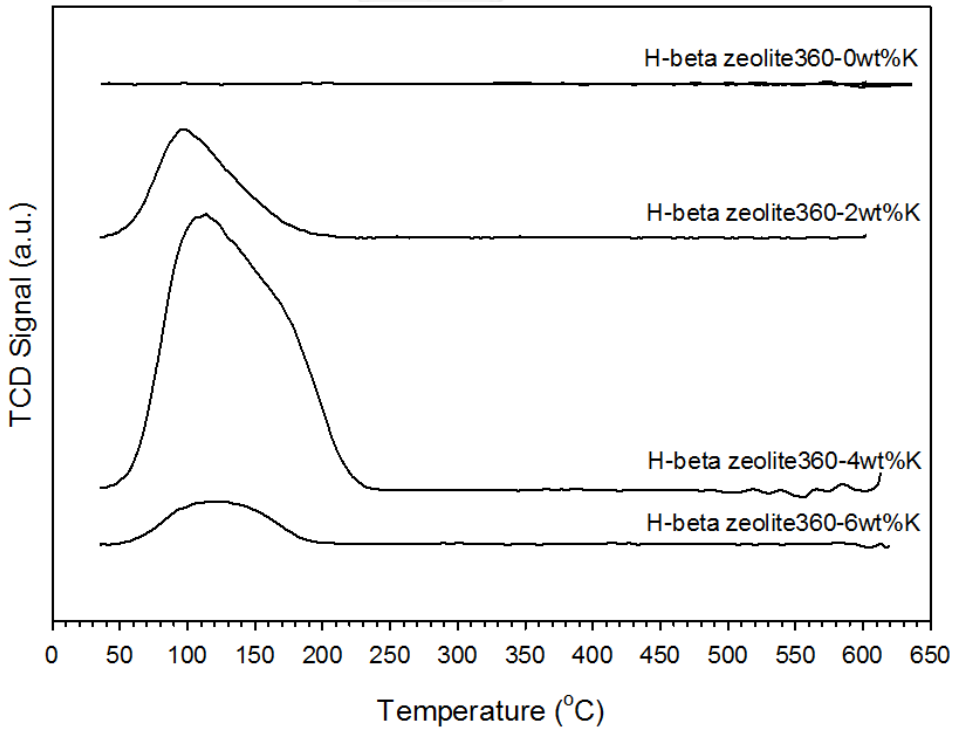

Figure 4. 6 The CO_2-TPD profile of H-beta zeolite and potassium modified H-beta zeolite catalyst.

As shown in Fig. 4.6, most of CO_2 was desorbed at temperature lower range 250 °C with maximum desorption peak at around 130 °C, indicating the weak basic site on surface potassium modified H-beta zeolite catalyst. Furthermore, the intensity of peak increased when the potassium loading are increased. This result, indicates that potassium loading can increase the basicity properties of H-beta zeolite catalysts as shown in Table 4.4, except H-beta zeolite360-6wt%K that intensity decrease due to the crystallinity structure of H-beta zeolite catalyst with potassium loading of 6wt%K. The structure collapsed detected by XRD indicates potassium oxide dislocate on amorphous surface of silica and alumina [46].

4.1.1.6 Thermal gravimetric and differential thermal analysis (TG-DTA).

The thermal analysis was used to study the carbon deposit of H-beta zeolite360 and potassium modified H-beta zeolite360 after being used in dehydration of lactic acid to acrylic acid. The weight loss of catalysts related with the combustion of carbon deposit.

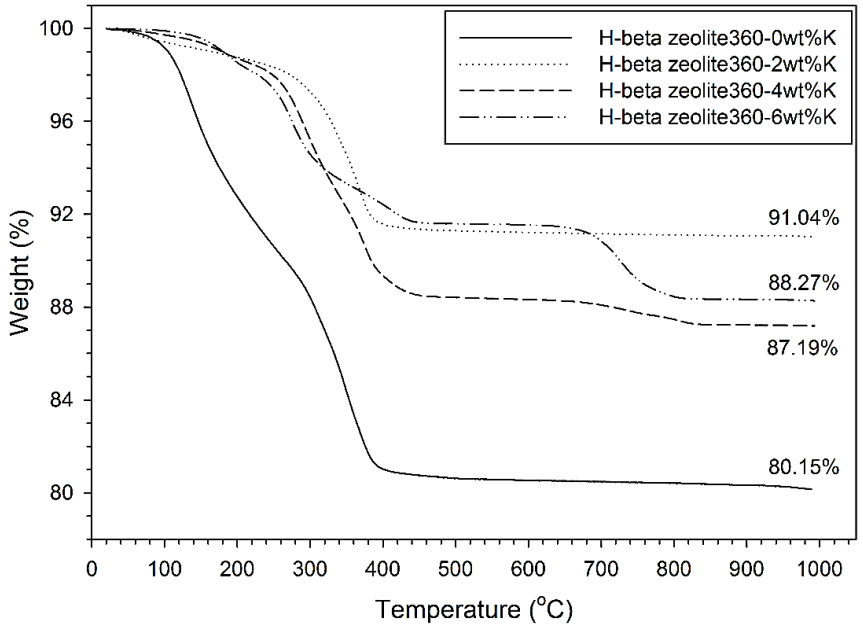

Figure 4. 7 The percent weight loss of potassium modified H-betazeolite360 catalysts after running reaction at reaction temperature 340 °C for 3 hr.

Figure 4.7 shown thermal gravimetric analysis of H-beta zeolite and potassium modified 2, 4 and 6 wt% on H-beta zeolite catalysts, the weight loss temperature of H-beta zeolite360-0 wt%K between 170 °C and 340 °C, at 170 °C may be assigned to the physically adsorbed water due to the mechanism reaction, water was generated. Furthermore, at 340 °C corresponding to coke deposit. While increase potassium loading 2, 4 and 6 wt%K had the same weight loss temperature was 340 °C except potassium loading 6 wt%K shown weight loss temperature in rang of 200 °C to 420 °C and at 730 °C that indicating, there were two kinds of coke deposit sites on the surface [17]. Moreover, the weight loss of H-beta zeolite was decreased when modified with potassium. These result demonstrated that potassium modification affect to decrease of coke deposit.

4.1.2 Dehydration of Lactic Acid Testing.

The activities of all the catalysts were tested in lactic acid dehydration reaction. Firstly, the catalyst 0.1 g was packed in glass reactor and preheated at the reaction temperature 340 °C for 1 hour with nitrogen gas flow rate 40 mL/min under atmospheric pressure. Then, the lactic acid solution with 34%volume was injected into the vaporizer with flowrate 1 ml/hr. and driven to reactor by nitrogen gas with flow rate 40 mL/min. Finally, The product (gas phase) was injected into the gas chromatograph with Flame Ionized Detector using DB-WAX capillary column.

The lactic acid conversion and the products selectivity in dehydration of lactic acid reaction at reaction time 120 minute are shown in Fig. 4.8 and Table 4.5

As shown in figure 4.8-4.12, when increase potassium loading 2, 4 and 6 wt% on H-beta zeolite catalyst, all of catalysts shown 100% lactic acid conversion and acrylic acid selectivity was about 0-43.8%. The H-beta zeolite360 catalyst with 4wt% potassium loading exhibited highest acrylic acid selectivity. The H-beta zeolite catalyst with 2-4 wt% potassium loading exhibited and elevation of acrylic acid and propionic acid selectivity, concurrently with the decrease of undesired product ,acetaldehyde, because potassium improve the acidity and basicity properties of catalyst surface. The decrease of acidity property caused the inhibition decarbonylation and decarboxylation reaction of lactic acid to acetaldehyde. At the same time, the increased of basicity property cause dehydration of lactic acid to acrylic acid and reduction of acrylic acid to propionic acid are generated [26]

These results, indicates potassium can promote the generation of acrylic acid and suppress the formation of acetaldehyde [16]. Moreover, at 6 wt% potassium loading, the selectivity of acrylic acid was decreased while selectivity of acetaldehyde increased when compared with 4wt% potassium loading due to the decrease of basicity property of catalyst surface that cause the increase of decarbonylation and decarboxylation to acetaldehyde is increased and dehydration of lactic acid to acrylic acid reaction is decreased.

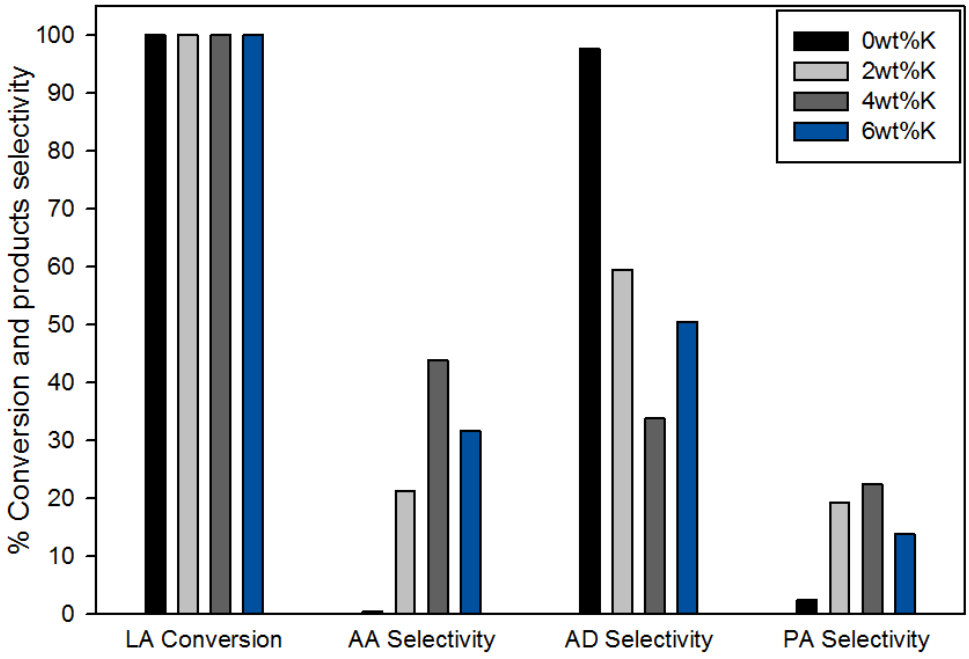

Figure 4. 8 The lactic acid conversion and products selectivity of H-beta zeolite and potassium modified H-beta zeolite catalysts at reaction temperature 340 °C and reaction time 120 minute. When AD, AA and PA are an acetaldehyde, acrylic acid and a propionic acid respectively.

Table 4. 5 The catalytic performance of potassium modified catalysts [a].

Catalysts.	LA. Conversion	Selectivity (%)		
		AD.	PA	AA
H-beta zeolite360-0wt%K	100	97.6	2.4	0.0
H-beta zeolite360-2wt%K	100	59.5	19.2	21.3
H-beta zeolite360-4wt%K	100	33.8	22.4	43.8
H-beta zeolite360-6wt%K	100	50.5	13.8	31.7

[a] reaction time 120 min.

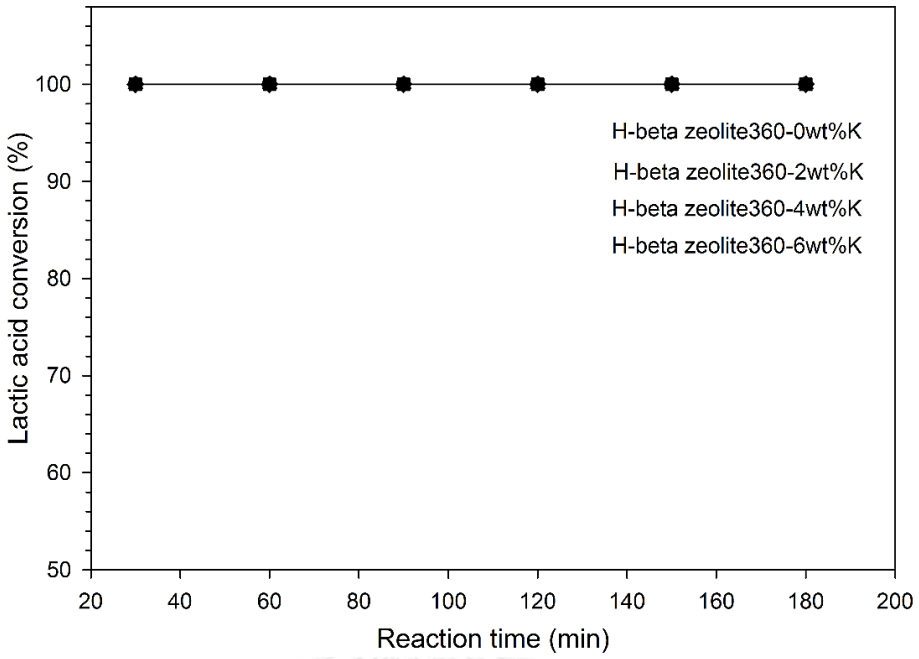

Figure 4. 9 The lactic acid conversion of H-beta zeolite and potassium modified H-beta zeolite catalysts at temperature 340 °C

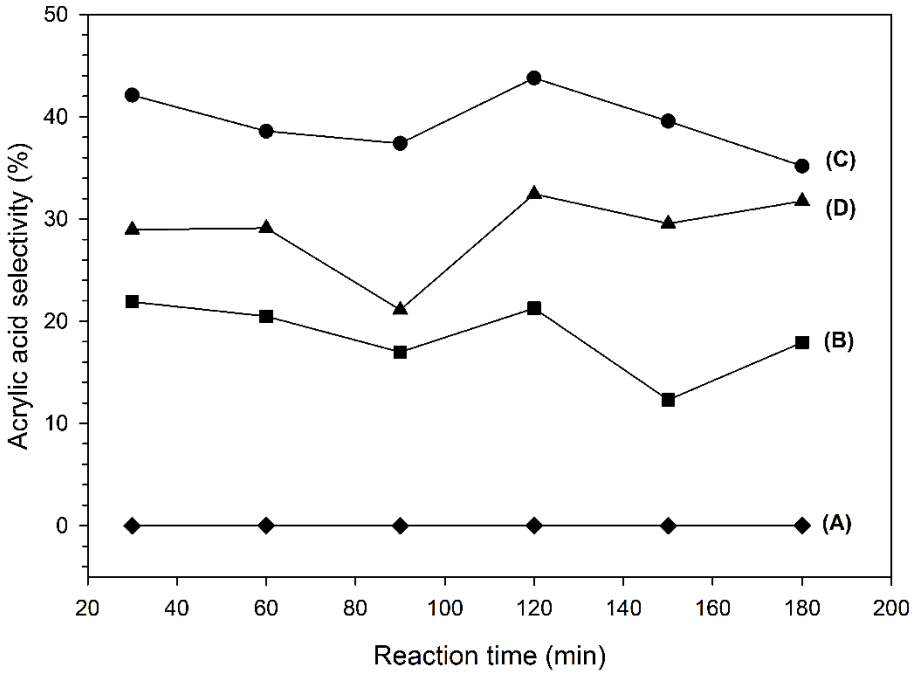

Figure 4. 10 The acrylic acid selectivity of H-beta zeolite and potassium modified H-beta zeolite catalysts at temperature 340 °C, (A), (B), (C) and (D) were potassium loading 0, 2, 4 and 6 wt%

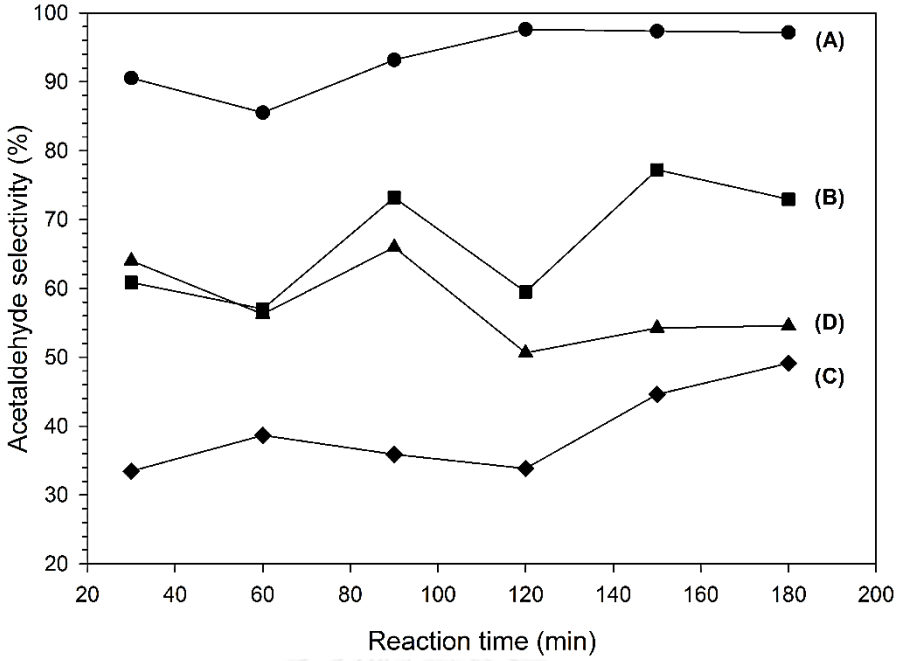

Figure 4. 11 The acetaldehyde selectivity of H-beta zeolite and potassium modified H-beta zeolite catalysts at temperature 340 °C, (A), (B), (C) and (D) were potassium loading 0, 2, 4 and 6 wt%

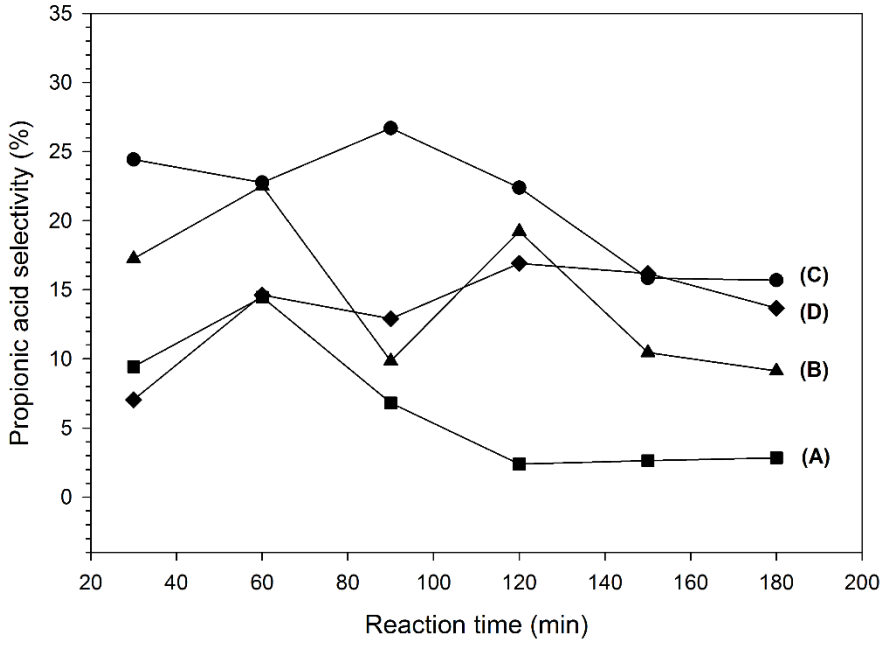

Figure 4. 12 The propionic acid selectivity of H-beta zeolite and potassium modified H-beta zeolite catalysts at temperature 340 °C, (A), (B), (C) and (D) were potassium loading 0, 2, 4 and 6 wt%

4.2 The effect of SiO_2/Al_2O_3 ratio of H-beta zeolite to catalytic activity

4.2.1 Characterization of Catalyst

4.2.1.1 Scanning electron microscopy (SEM) and energy x-ray spectroscopy (EDX)

The morphology and elemental composition over the catalysts surface were determined by scanning electron microscope (SEM) and energy X-ray spectroscopy (EDX), respectively. The SEM model is JEOL mode JSM-5800LV and Link Isis Series 300 program was performed for EDX.

Table 4. 6 The element composition of modified H-beta zeolite catalysts with potassium loading of 4 wt% from energy X-ray spectroscopy

Catalysts	Weight%			
	O	Al	Si	K
H-beta Zeolite40-4wt%K	39.25	2.83	53.19	4.73
H-beta Zeolite360-4wt%K	49.36	0.95	45.44	4.25
H-beta Zeolite500-4wt%K	47.09	0.81	47.98	4.12

The element compositions of H-beta zeolite catalyst with SiO_2/Al_2O_3 ratios of 40, 360 and 500 and 4wt% potassium loading are shown in Table 4.6, it has been found that the values of potassium composition analyzed by energy X-ray spectroscopy (EDX) were higher than these calculated for each sample. This may be due to the potassium composition from energy X-ray spectroscopy (EDX) is potassium composition at surface catalyst only.

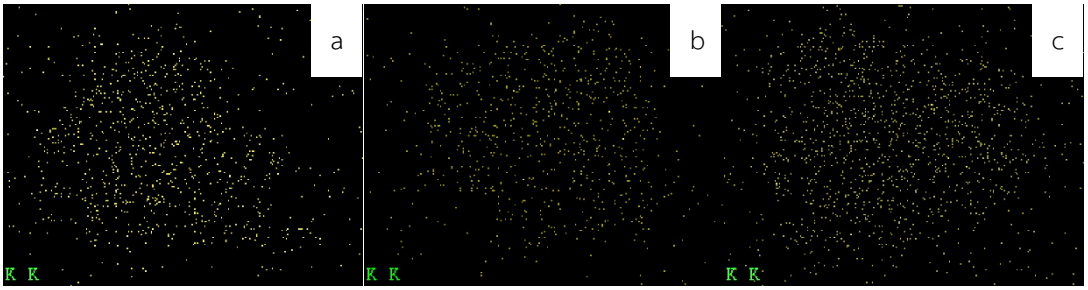

Figure 4. 13 Potassium distribution on surface catalysts: (a) H-beta zeolite40-4wt%K, (b) H-beta zeolite360-4wt%K and (c) H-beta zeolite500-4wt%K

The potassium distribution on surface of H-beta zeolite with 4 wt% loading potassium is presented in Fig. 4.13, it has been shown that potassium can be dispersed on surface of H-beta zeolite catalyst. The scanning electron microscopy of potassium modified H-beta zeolite with 4 wt% potassium loading is presented in Fig. 4.14, indicating that the morphology of crystalline of all catalysts have spherical shape and the particle size distribution is a narrow distribution.

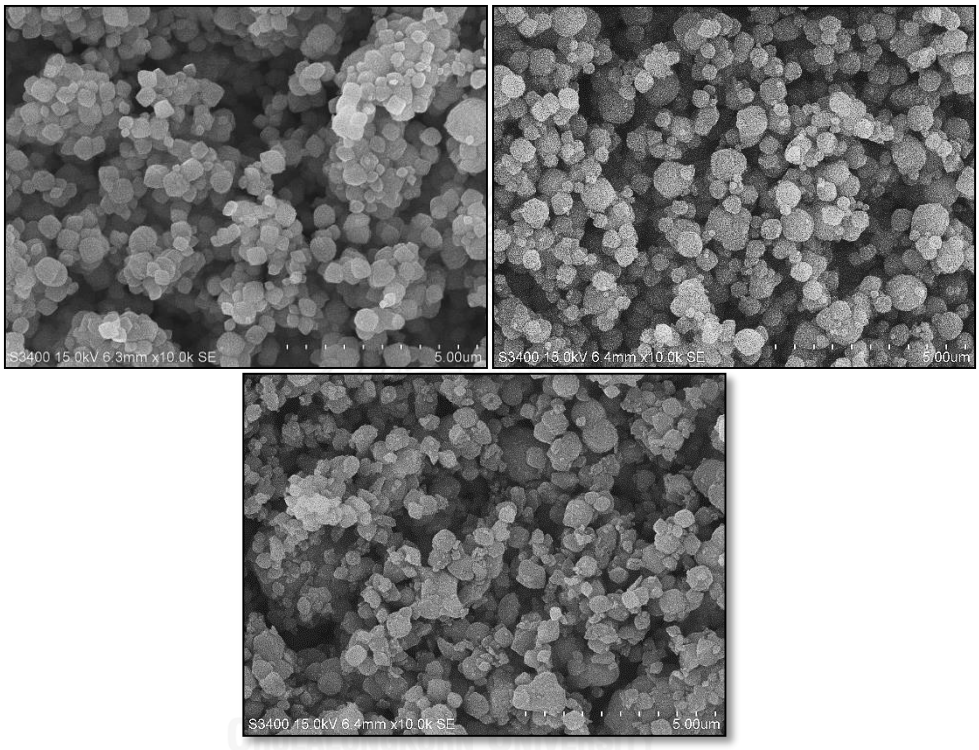

Figure 4. 14 The SEM images of all catalysts: (a) H-beta zeolite40-4wt%K, (b) H-beta zeolite360-4wt%K and (c) H-beta zeolite500 4wt%K

4.2.1.2 X-Ray Diffraction (XRD)

The X-ray diffraction (XRD) patterns of potassium modified H-beta zeolite catalysts with 4wt% potassium loading were measured by the SIEMENS D5000 X-ray diffractometer with a Cu K_α radiation source. The XRD patterns were collected with the 2θ in range of 10 to 70 degree with rate of 2.5 degree/min.

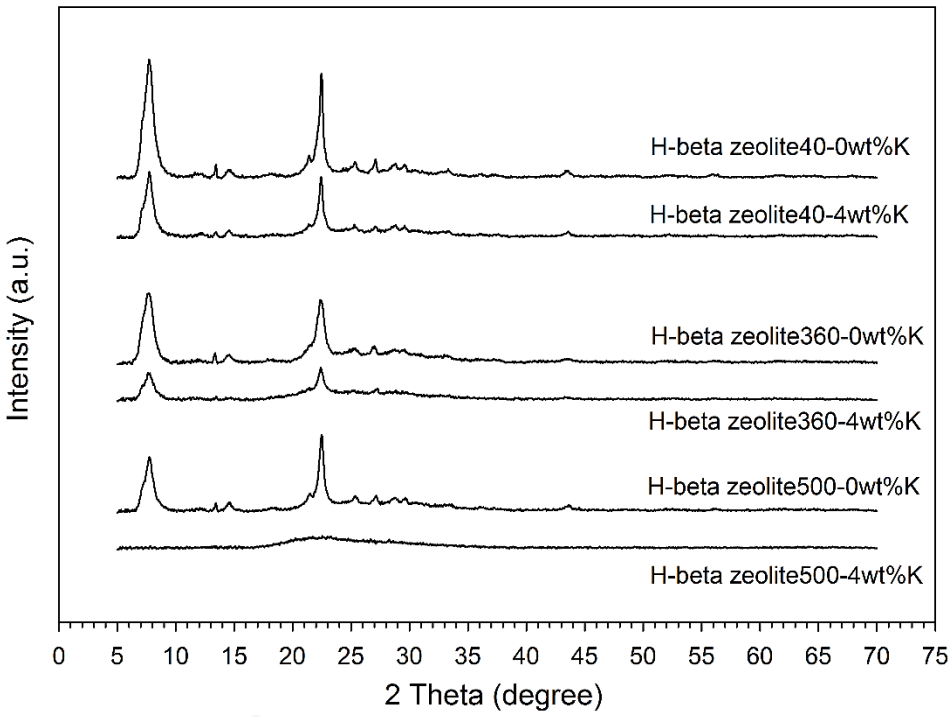

Figure 4. 15 The XRD pattern of modified H-beta zeolite catalysts with potassium loading 4 wt%.

The X-ray diffraction (XRD) patterns of potassium modified H-beta zeolite catalysts with 4wt% potassium loading are presented in Fig. 4.15, it has been shown that the characteristic peaks of H-beta zeolite catalyst in the 2θ range of 5-70 degree were 7.8, 16.5, 22.5, 25.3, 26.9, 29.5 and 43.5 degree [46]. As shown in Fig. 4.15, all of the H-beta zeolite catalysts with 4wt% potassium loading except H-beta zeolite500-4wt%K, retained the characteristic peaks of H-beta zeolite, indicating that they retained the basic structure of H-beta zeolite catalyst. On the other hand, the intensities of these peaks decreased when SiO_2/Al_2O_3 ratios of H-beta zeolite catalysts were increased, indicating that the framework structure was partially destroyed with the

increasing SiO_2/Al_2O_3 ratios due to dealumination or desilication [44]. The framework structure of H-beta zeolite was destroyed due to potassium affecting an increased hydrolysis of Si-O-Al. Moreover, potassium oxide caused the decrease of thermal stability of H-beta zeolite. The deterioration and collapse of the framework structure of catalysts were formed during the calcination at high temperature, as shown in Fig. 4.16

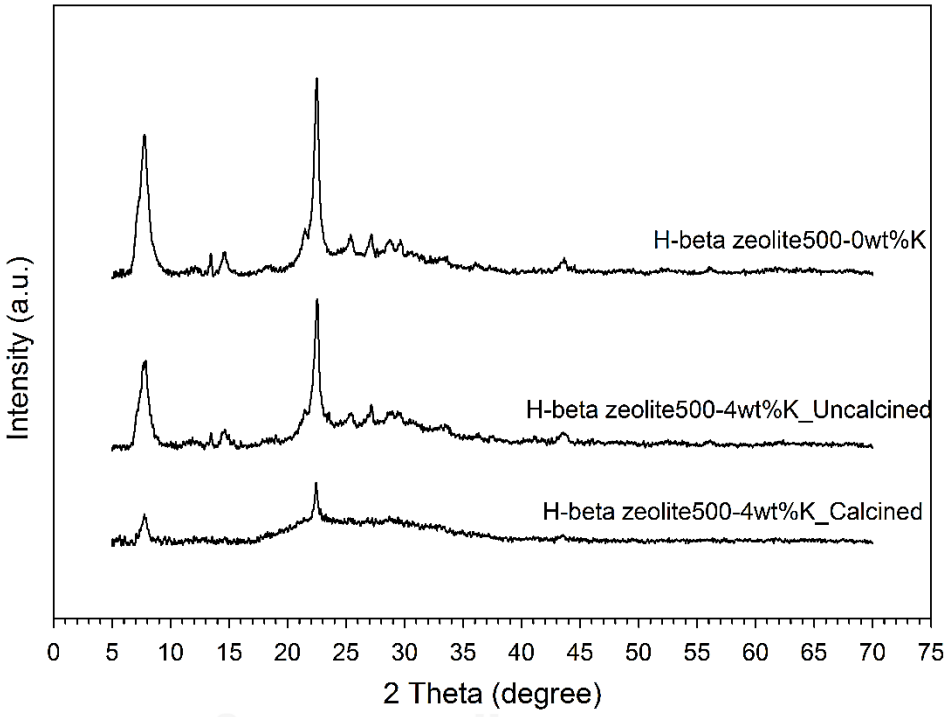

Figure 4. 16 The effect of potassium and temperature on framework structure of H-beta zeolite500

4.2.1.3 Nitrogen physisorption

The nitrogen adsorption-desorption isotherms of potassium modified H-beta zeolite catalysts with 4wt% potassium loading are shown in Fig. 4.17 while the surface area of catalysts were measured by N_2-physisorption and the results are shown in Table 4.7.

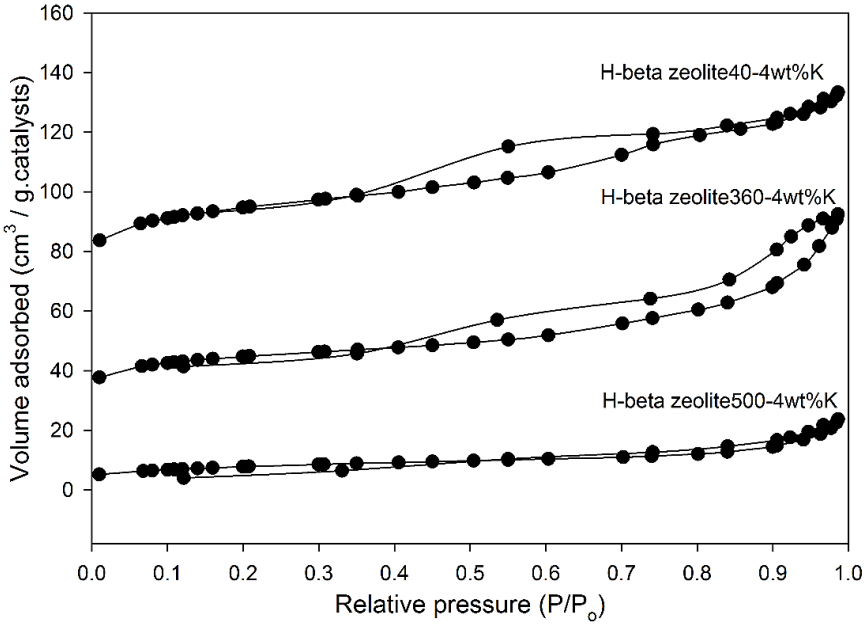

Figure 4. 17 The nitrogen adsorption-desorption isotherm of modified H-beta zeolite catalysts with potassium loading 4 wt%.

Table 4. 7 The physical properties of modified H-beta zeolite catalysts with potassium loading 4 wt%.

Catalyst	Surface area* (m^2/g)	Micropore volume** (cm^3/g)	Average pore size*** (nm)
H-beta zeolite40-4wt%K	320	0.111	2.6
H-beta zeolite360-4wt%K	152	0.047	3.7
H-beta zeolite500-4wt%K	28	0.002	5.0

*The surface area was calculated by Brunauer–Emmett–Teller (BET) method.

**The micropore volume was evaluated by t-plot method.

***The average pore size was evaluated by adsorption average pore width (4V/A BET).

As shown in Fig. 4.17, when loading potassium 4 wt% on H-beta zeolite catalyst with varying SiO_2/Al_2O_3 ratios (40, 360 and 500), All the catalysts showed nitrogen adsorption-desorption isotherm type IV. The hysteresis loop indicated the multiple range of physisorption isotherm, associated with the filling and emptying of mesopore of surface catalysts.

The surface areas of catalysts were measured by N_2-physisorption and the results are shown in Table 4.7, with the decreasing aluminum content in H-beta zeolite catalysts or increasing SiO_2/Al_2O_3 ratios, surface area and micropore volume of H-beta zeolite catalysts were decreased from 320 to 28 m^2/g and from 0.111 to 0.002 cm^3/g respectively, while the average pore size of catalysts was increased from 2.6 to 5.0 nm due to the increase of SiO_2/Al_2O_3 ratios affecting an increase of dealumination that caused the increase of destruction of framework structure of H-beta zeolite catalysts.

4.2.1.4 Ammonia temperature-programmed desorption (NH_3-TPD)

The acid properties of catalyst are widely characterized by ammonia temperature-programmed desorption (NH_3-TPD). The NH_3-TPD profiles of H-beta zeolite catalyst and potassium modified H-beta zeolite catalyst are present in Fig. 4.18, while acid properties of modified H-beta zeolite catalyst are shown in Table 4.8

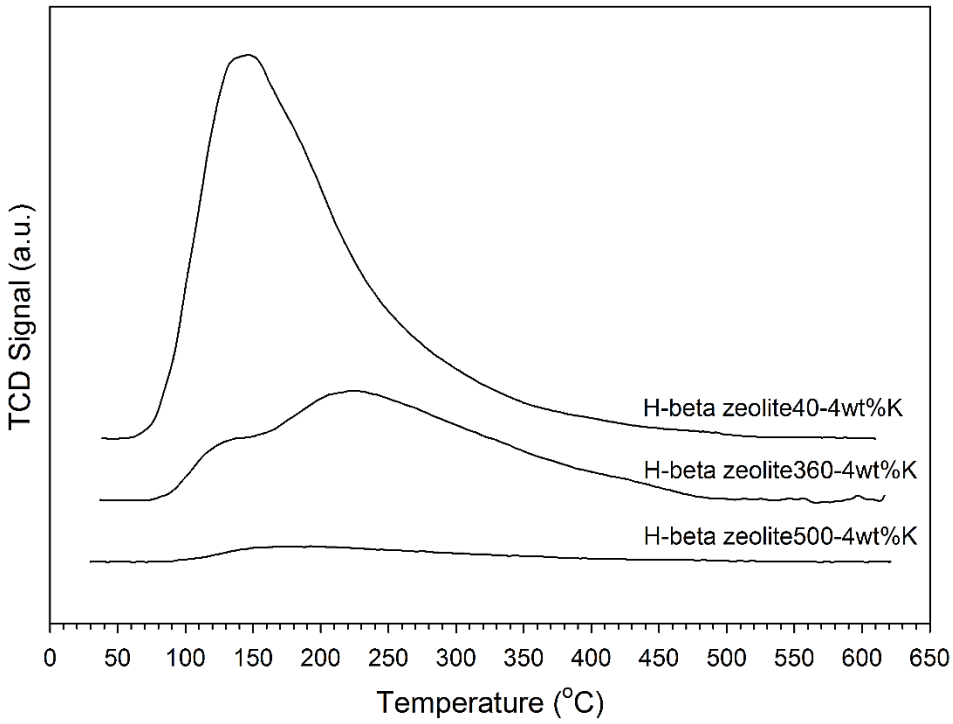

Figure 4. 18 The NH_3-TPD profile of modified H-beta zeolite catalysts with potassium loading 4 wt%.

Table 4. 8 The acidity properties of modified H-beta zeolite catalysts with potassium loading 4 wt%.

Catalysts	acid strength		Total acid
	weak	medium & strong	(mmol NH_3/g cat.)
H-beta Zeolite40-4wt%K	0.064	0.025	0.091
H-beta Zeolite360-4wt%K	0.023	0.010	0.033
H-beta Zeolite500-4wt%K	0.008	0.004	0.012

The acid strength of catalyst relates with the desorption temperature of ammonia [47]. Furthermore, the amount of total acidity relates with the total amount ammonia desorption [48]. The desorption of ammonia within the range of temperature lower than 250 °C was attributed to weak acid site and that within the range of temperature higher than 250 °C was attributed to medium and strong acid site on catalyst surface [49]. As shown in Fig. 4.18, with the increasing SiO_2/Al_2O_3 ratios of 40, 360 and 500 of H-beta zeolite catalysts, the area of peak was decreased, indicating the decrease of acid site on catalyst surface occurred when increasing SiO_2/Al_2O_3 ratios due to acid property of aluminum in H-beta zeolite catalysts. These results indicate that the increasing SiO_2/Al_2O_3 ratios affects the decreased of acid properties of H-beta zeolite catalysts.

4.2.1.5 Carbon dioxide temperature-programmed desorption (CO_2-TPD)

The basic properties of catalyst are widely characterized by carbondioxide temperature-programmed desorption (CO_2-TPD). The amount of total basicity relates with the total amount of carbondioxide desorption. The CO_2-TPD profiles of H-beta zeolite catalyst and potassium modified H-beta zeolite catalyst are shown in Fig. 4.19, while the data of TPD of desorbed CO_2 is shown in Table 4.9

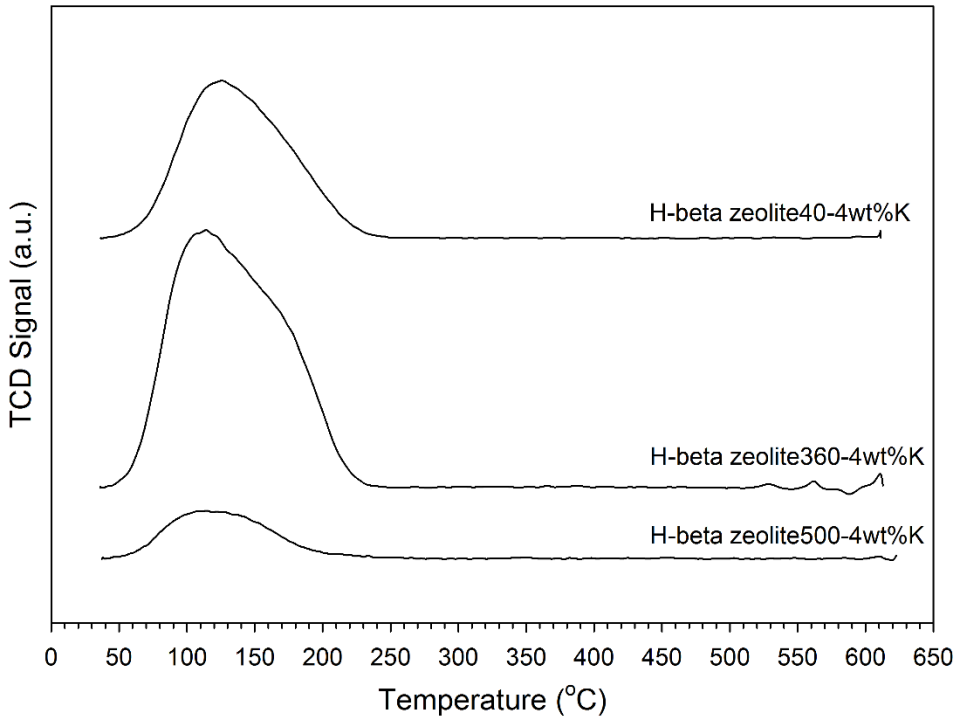

Figure 4. 19 The CO_2-TPD profile of modified H-beta zeolite catalysts with potassium loading 4 wt%.

Table 4. 9 The basicity properties of modified H-beta zeolite catalysts with potassium loading 4 wt%.

Catalysts	Total Base (umol CO_2/g cat.)
H-beta Zeolite40-4wt%K	7.574
H-beta Zeolite360-4wt%K	15.950
H-beta Zeolite500-4wt%K	2.297

As shown in Fig. 4.19, when loading potassium 4 wt% on H-beta zeolite catalyst with increasing SiO_2/Al_2O_3 ratios of 40, 360 and 500, most of adsorbed CO_2 was desorbed at temperature lower 250 °C with maximum desorption peak at around 130 °C, indicating the weak basic site on surface of potassium modified H-beta zeolite catalysts. Furthermore, the area of peak increased when increasing SiO_2/Al_2O_3 ratios from 40 to 360, indicating the increase of basic site of catalyst. On the other hand, the area of peak decreased when increasing SiO_2/Al_2O_3 ratios from 360 to 500, indicating the decrease of basic site of catalyst due to potassium addition of H-beta zeolite catalysts, probable forming alkali metal-aluminosilicate with aluminum [46]. The decrease of aluminum content in H-beta zeolite affects the decreased interaction between potassium and aluminum. These result caused the increased basicity property of H-beta zeolite when increasing SiO_2/Al_2O_3 ratio from 40 to 360. As for the decrease of catalyst basicity when increasing SiO_2/Al_2O_3 ratios from 360 to 500 might be attributed to destroy of the framework structure probably due to high SiO_2/Al_2O_3 ratios of 500.

4.2.1.6 Thermal gravimetric and differential thermal analysis (TG-DTA).

The thermal analysis was used to study the carbon deposit of potassium modified H-beta zeolite catalysts with 4wt% potassium loading after being used in dehydration of lactic acid to acrylic acid. The weight loss of catalysts relate with the combustion of carbon deposit.

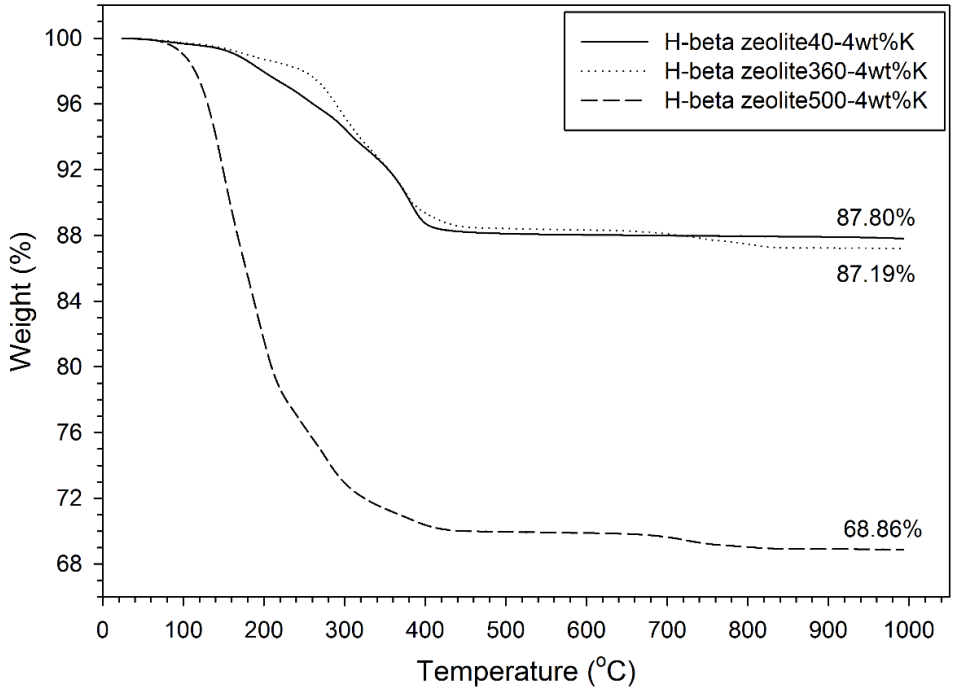

Figure 4. 20 The percent weight loss of loading potassium 4 wt% on H-beta zeolite catalyst with increase SiO_2/Al_2O_3 ratio 40, 360 and 500 after running reaction at reaction temperature 340 °C for 3 hr.

Fig. 4.20 showed thermal gravimetric analysis of loading potassium 4 wt% on H-beta zeolite catalyst with increasing SiO_2/Al_2O_3 ratios of 40, 360 and 500 after running lactic acid dehydration reaction at reaction temperature 340 °C for 3 hr. The weight loss temperature of loading potassium 4wt% of H-beta zeolite with SiO_2/Al_2O_3 ratio 40 and 360 appeared during the range of 200 °C to 420 °C and total weight loss 17%. While loading potassium 4wt% of H-beta zeolite with SiO_2/Al_2O_3 ratio 500 exhibited weight loss temperature during the range of 120 °C to 420 °C and total weight 32%. The weight loss temperature shifted to lower temperature and increased total weight loss indicate the increase of coke deposition of catalysts.

4.2.2 Dehydration of Lactic Acid Testing.

The activity of all catalyst was tested in lactic acid dehydration reaction. Firstly, the catalyst 0.1 g was packed in glass reactor and preheated at the reaction temperature 340 ºC for 1 hour with nitrogen gas flow rate 40 mL/min under atmospheric pressure. Then, the lactic acid solution 34%volume was injected into the vaporizer with flowrate 1 ml/hr. and driven to reactor by nitrogen gas with flow rate 40 mL/min. Finally, The product (gas phase) was injected into the gas chromatograph with Flame Ionized Detector using DB-WAX capillary column.

The lactic acid conversion and the products selectivity in dehydration of lactic acid reaction at reaction time 120 minute are shown in Fig. 4.21 and Table 4.10

As shown in Fig.4.21-4.25, with the increasing SiO_2/Al_2O_3 ratios of 40, 360 and 500 on H-beta zeolite modified with 4wt% potassium loading, all of catalysts exhibit 100% lactic acid conversion and acrylic acid selectivity was about 0-43.8%. The modification made with 4wt% potassium loading of H-beta zeolite with SiO_2/Al_2O_3 ratio 360 catalyst exhibited highest acrylic acid selectivity. Whereas, the modification made with 4wt% potassium loading of H-beta zeolite with SiO_2/Al_2O_3 ratio 40 and 500 catalysts exhibited the same acrylic acid (13.2% and 12.7%) and acetaldehyde selectivities (81.6 and 84.6%). Furthermore, the propionic acid selectivity of H-beta zeolite40-4wt%K was more than that of H-beta zeolite500-4wt%K, corresponding to the decrease of basic property of catalysts due to the acidity property of catalysts were decreased and the basicity property of catalysts were increased when increasing SiO_2/Al_2O_3 ratio from 40 to 360. In addition, the decrease of acetaldehyde selectivity and the increase of acrylic acid selectivity were also affected. While, increasing SiO_2/Al_2O_3 ratio from 360 to 500, the basicity of catalysts were decreased due to collapse of the framework structure of catalysts, affecting the decrease of acrylic acid selectivity.

These results indicate that the different SiO_2/Al_2O_3 ratios on H-beta zeolite catalyst had an influence on the catalytic performance. The lower SiO_2/Al_2O_3 ratio, the

higher acidic property. While the excessively high SiO_2/Al_2O_3 ratio may cause the collapse of framework structure of catalysts. So, the H-beta zeolite to be used on lactic acid dehydration reaction should have suitable SiO_2/Al_2O_3 ratio.

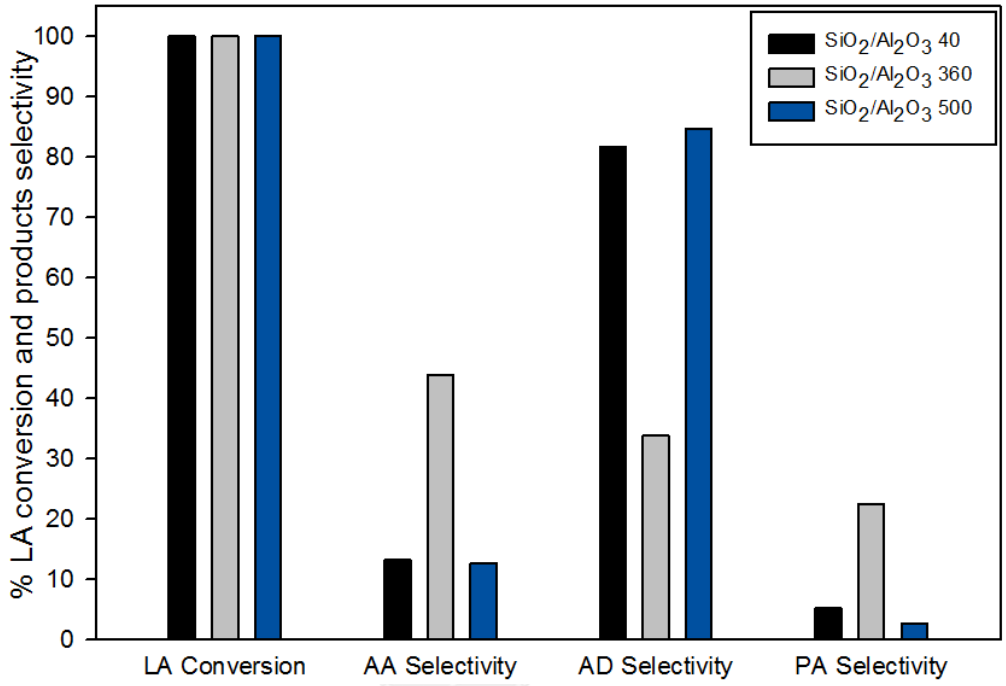

Figure 4. 21 The lactic acid conversion and products selectivity of loading 4wt%K on H-beta zeolite catalyst after run reaction temperature 340 °C and reaction time 120 minute. When AD, AA and PA are an acetaldehyde, acrylic acid and a propionic acid respectively.

Table 4. 10 The catalytic performance of potassium modified catalysts [a].

Catalysts.	LA. Conversion	Selectivity (%)		
		AD.	PA	AA
H-beta zeolite40-4wt%K	100	81.6	5.2	13.2
H-beta zeolite360-4wt%K	100	33.8	22.4	43.8
H-beta zeolite500-4wt%K	100	84.6	2.7	12.7

[a] reaction time 120 min.

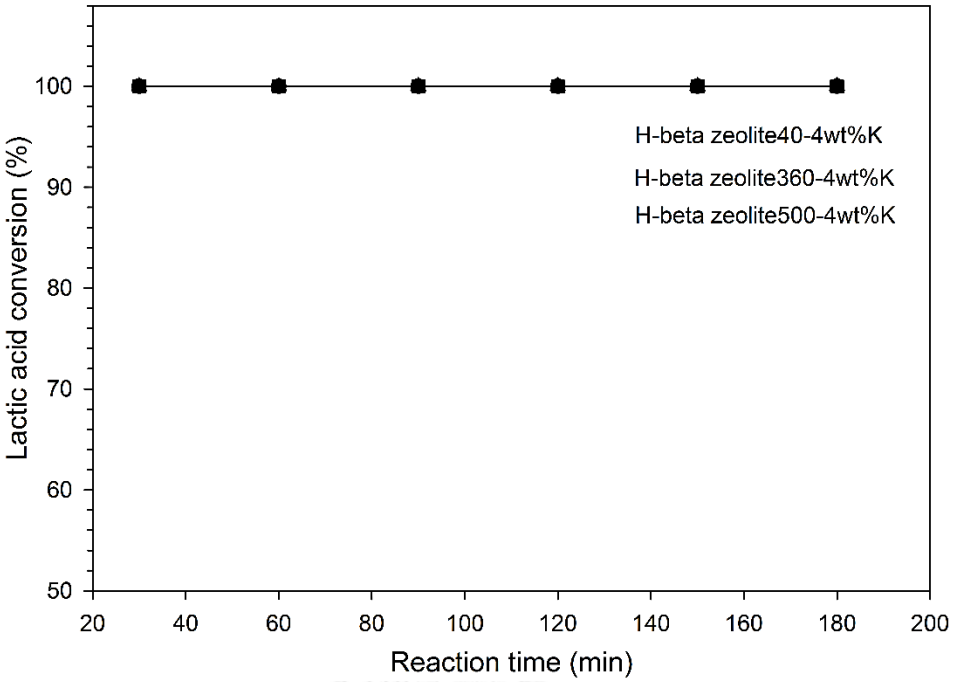

Figure 4. 22 The lactic acid conversion of loading 4wt%K on H-beta zeolite catalysts after run reaction temperature 340 °C and reaction time 120 minute.

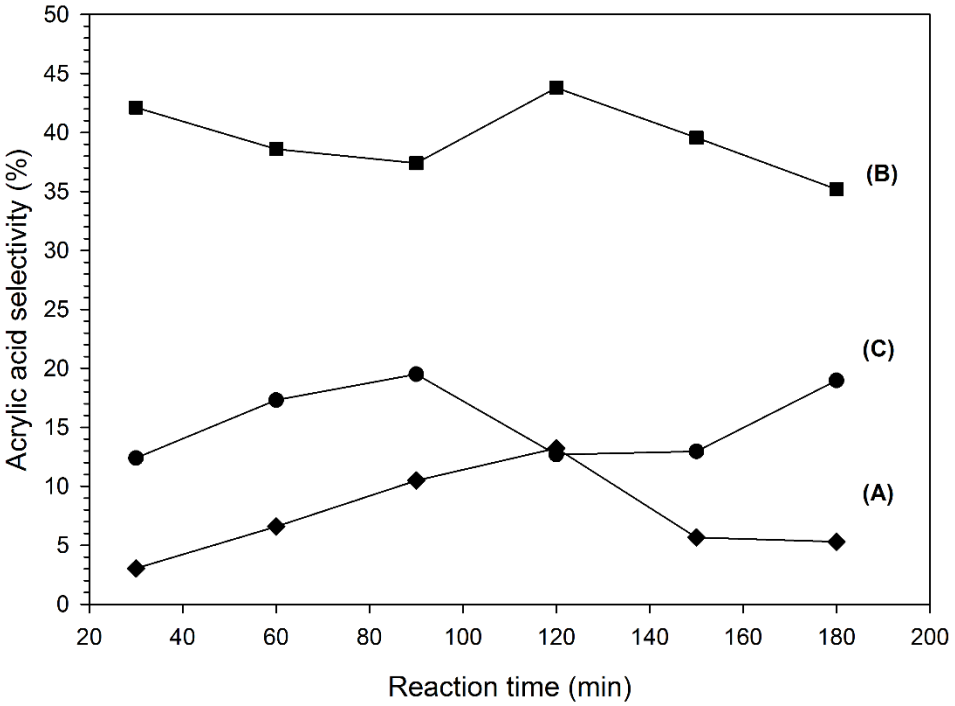

Figure 4. 23 The acrylic acid selectivity of loading 4wt%K on H-beta zeolite catalysts after run reaction temperature 340 °C, when (A), (B) and (C) were SiO_2/Al_2O_3 ratio 40, 360 and 500 respectively.

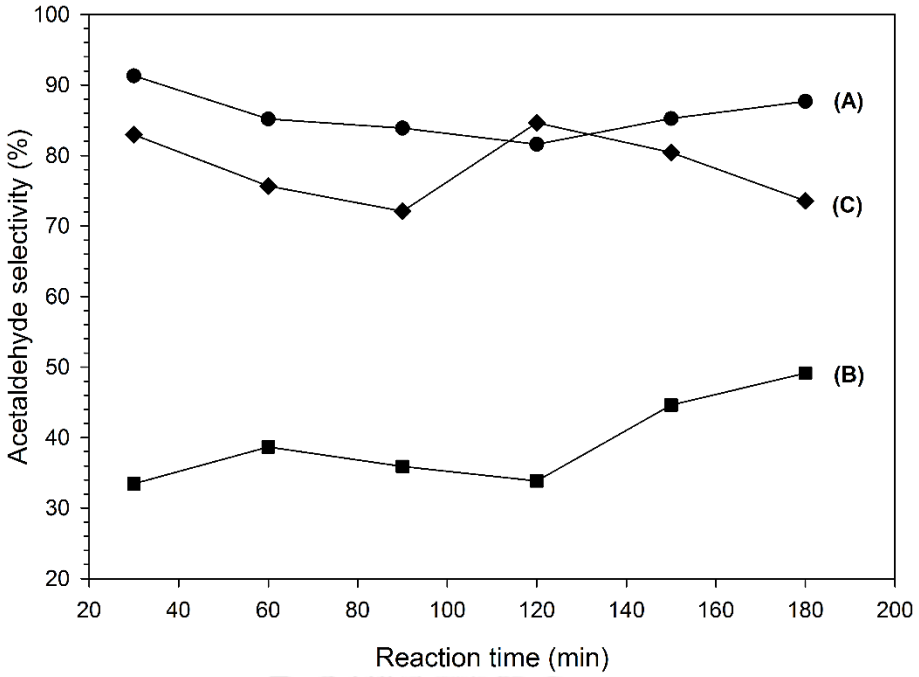

Figure 4. 24 The acetaldehyde selectivity of loading 4wt%K on H-beta zeolite catalysts after run reaction temperature 340 °C, when (A), (B) and (C) were SiO_2/Al_2O_3 ratio 40, 360 and 500 respectively.

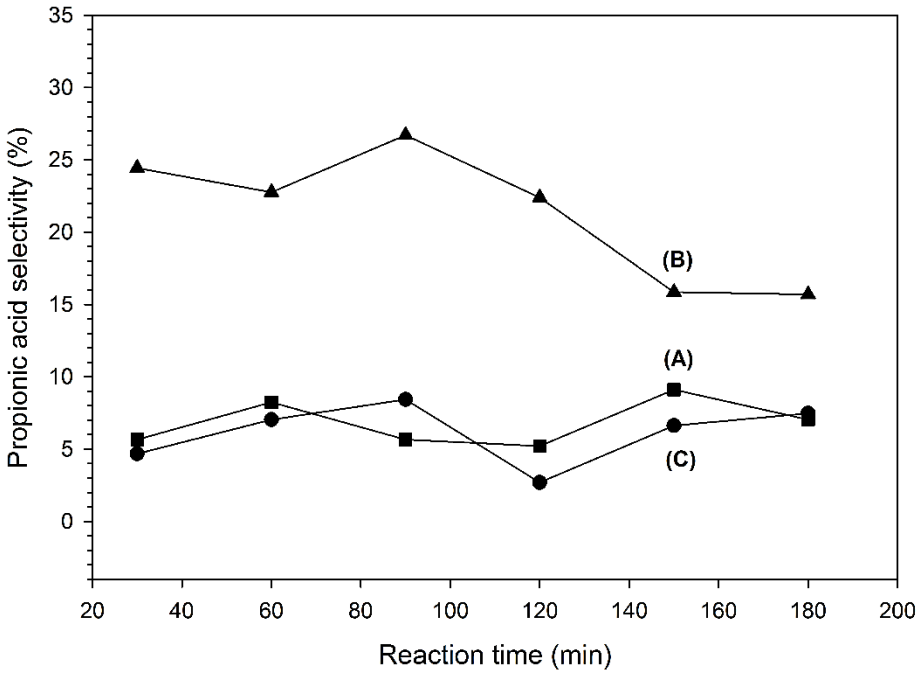

Figure 4. 25 The propionic acid selectivity of loading 4wt%K on H-beta zeolite catalysts after run reaction temperature 340 °C, when (A), (B) and (C) were SiO_2/Al_2O_3 ratio 40, 360 and 500 respectively.

CHAPTER V
CONCLUSIONS

5.1 Conclusions

In this research, the effect of different potassium loading (2, 4 and 6 wt %) and the effect of SiO_2/Al_2O_3 ratios (40, 360 and 500) on H-beta zeolite catalysts were studied. The modified H-beta zeolite catalyst with 4wt% potassium loading was selected to study effect of SiO_2/Al_2O_3 ratios on H-beta zeolite catalysts. The results can be concluded as follows:

1. Potassium can improve the acidity and basicity properties of H-beta zeolite catalysts and tends to promote the generation of acrylic acid and suppress the formation of acetaldehyde.

2. The ratio of SiO_2/Al_2O_3 on H-beta zeolite catalysts affected the catalytic performance. The catalysts with lower SiO_2/Al_2O_3 ratio, contributing to more acidic property caused the decrease of acrylic acid selectivity and increase of acetaldehyde selectivity. The catalysts with very high SiO_2/Al_2O_3 ratio adversely affected the decrease of acrylic acid selectivity, probably due to the structural collapse of catalyst framework. In this study, the H-beta zeolite with SiO_2/Al_2O_3 ratio of 360 exhibited the highest catalytic performance when compared with H-beta zeolite catalysts having SiO_2/Al_2O_3 ratios of 40 and 500.

5.2 Recommendation

1. The difference synthesis method of catalysts should be affect to catalytic performance of catalyst.

2. The calcination temperature of catalysts should be affect to crystallinity structure of catalysts that should be effect to catalytic performance of catalyst.

3. The type of zeolite should be affect to catalytic performance of catalyst.

REFERENCES

[1] Buchanan, G. Increasing feedstock production for biofuels: economic drivers, environmental implications, and the role of research. DIANE Publishing, 2010.

[2] Gao, C., Ma, C., and Xu, P. Biotechnological routes based on lactic acid production from biomass. Biotechnol Adv 29(6) (2011): 930-9.

[3] John, R.P., G, S.A., Nampoothiri, K.M., and Pandey, A. Direct lactic acid fermentation: focus on simultaneous saccharification and lactic acid production. Biotechnol Adv 27(2) (2009): 145-52.

[4] Hama, S., et al. Production of d-lactic acid from hardwood pulp by mechanical milling followed by simultaneous saccharification and fermentation using metabolically engineered Lactobacillus plantarum. Bioresour Technol 187 (2015): 167-172.

[5] Mimitsuka, T., et al. Production of D-lactic acid in a continuous membrane integrated fermentation reactor by genetically modified Saccharomyces cerevisiae: enhancement in D-lactic acid carbon yield. J Biosci Bioeng 119(1) (2015): 65-71.

[6] Castillo Martinez, F.A., Balciunas, E.M., Salgado, J.M., Domínguez González, J.M., Converti, A., and Oliveira, R.P.d.S. Lactic acid properties, applications and production: A review. Trends in Food Science & Technology 30(1) (2013): 70-83.

[7] Dusselier, M., Van Wouwe, P., Dewaele, A., Makshina, E., and Sels, B.F. Lactic acid as a platform chemical in the biobased economy: the role of chemocatalysis. Energy & Environmental Science 6(5) (2013): 1415.

[8] Maki-Arvela, P., Simakova, I.L., Salmi, T., and Murzin, D.Y. Production of lactic acid/lactates from biomass and their catalytic transformations to commodities. Chem Rev 114(3) (2014): 1909-71.

[9] Fan, Y., Zhou, C., and Zhu, X. Selective Catalysis of Lactic Acid to Produce Commodity Chemicals. Catalysis Reviews 51(3) (2009): 293-324.

[10] Datta, R. and Henry, M. Lactic acid: recent advances in products, processes and technologies — a review. Journal of Chemical Technology & Biotechnology 81(7) (2006): 1119-1129.

[11] Bettahar, M., Costentin, G., Savary, L., and Lavalley, J. On the partial oxidation of propane and propylene on mixed metal oxide catalysts. Applied Catalysis A: General 145(1) (1996): 1-48.

[12] Culp, A., Holmes, K., Nagrath, R., and Nessenson, D. Propane to Acrylic Acid. (2013).

[13] Lin, M.M. Selective oxidation of propane to acrylic acid with molecular oxygen. Applied Catalysis A: General 207(1) (2001): 1-16.

[14] Landi, G., Lisi, L., and Russo, G. Oxidation of propane and propylene to acrylic acid over vanadyl pyrophosphate. Journal of Molecular Catalysis A: Chemical 239(1-2) (2005): 172-179.

[15] Zhang, J., Zhao, Y., Pan, M., Feng, X., Ji, W., and Au, C.-T. Efficient Acrylic Acid Production through Bio Lactic Acid Dehydration over NaY Zeolite Modified by Alkali Phosphates. ACS Catalysis 1(1) (2011): 32-41.

[16] Zhang, X., Lin, L., Zhang, T., Liu, H., and Zhang, X. Catalytic dehydration of lactic acid to acrylic acid over modified ZSM-5 catalysts. Chemical Engineering Journal 284 (2016): 934-941.

[17] Sun, P., et al. Potassium modified NaY: A selective and durable catalyst for dehydration of lactic acid to acrylic acid. Catalysis Communications 10(9) (2009): 1345-1349.

[18] Blanco, E., Delichere, P., Millet, J.M.M., and Loridant, S. Gas phase dehydration of lactic acid to acrylic acid over alkaline-earth phosphates catalysts. Catalysis Today 226 (2014): 185-191.

[19] ZHANG, J., Jianping, L., Xiaobo, X., and Peilin, C. Evaluation of catalysts and optimization of reaction conditions for the dehydration of methyl lactate to acrylates. Chinese Journal of Chemical Engineering 16(2) (2008): 263-269.

[20] Yuan, C., Liu, H., Zhang, Z., Lu, H., Zhu, Q., and Chen, Y. Alkali-metal-modified ZSM-5 zeolites for improvement of catalytic dehydration of lactic acid to acrylic acid. Chinese Journal of Catalysis 36(11) (2015): 1861-1866.

[21] Yan, J., Yu, D., Sun, P., and Huang, H. Alkaline Earth Metal Modified NaY for Lactic Acid Dehydration to Acrylic Acid: Effect of Basic Sites on the Catalytic Performance. Chinese Journal of Catalysis 32(3-4) (2011): 405-411.

[22] Corma, A. State of the art and future challenges of zeolites as catalysts. Journal of Catalysis 216(1-2) (2003): 298-312.

[23] Yan, B., Mahmood, A., Liang, Y., and Xu, B.-Q. Sustainable production of acrylic acid: Rb+-and Cs+-exchanged Beta zeolite catalysts for catalytic gas-phase dehydration of lactic acid. Catalysis Today 269 (2016): 65-73.

[24] Martinez, F.A.C., Balciunas, E.M., Salgado, J.M., González, J.M.D., Converti, A., and de Souza Oliveira, R.P. Lactic acid properties, applications and production: a review. Trends in Food Science & Technology 30(1) (2013): 70-83.

[25] Lin, M., Desai, T.B., Kaiser, F.W., and Klugherz, P.D. Reaction pathways in the selective oxidation of propane over a mixed metal oxide catalyst. Catalysis Today 61(1) (2000): 223-229.

[26] Näfe, G., et al. Deactivation behavior of alkali-metal zeolites in the dehydration of lactic acid to acrylic acid. Journal of Catalysis 329 (2015): 413-424.

[27] Sun, P., Yu, D., Tang, Z., Li, H., and Huang, H. NaY zeolites catalyze dehydration of lactic acid to acrylic acid: studies on the effects of anions in potassium salts. Industrial & Engineering Chemistry Research 49(19) (2010): 9082-9087.

[28] Weitkamp, J. Zeolites and catalysis. Solid State Ionics 131(1) (2000): 175-188.

[29] Stöcker, M. Gas phase catalysis by zeolites. Microporous and mesoporous materials 82(3) (2005): 257-292.

[30] Corma, A. State of the art and future challenges of zeolites as catalysts. Journal of Catalysis 216(1) (2003): 298-312.

[31] Baerlocher, C., McCusker, L.B., and Olson, D.H. Atlas of zeolite framework types. Elsevier, 2007.

[32] Akbar, S. Characterization of Beta Zeolites by X-Ray Diffraction, Scanning Electron Microscope, and Refractive Index Techniques. (2010).

[33] Hegde, S., Kumar, R., Bhat, R., and Ratnasamy, P. Characterization of the acidity of zeolite Beta by FTi. r. spectroscopy and tpd of NH 3. Zeolites 9(3) (1989): 231-237.

[34] Higgins, J., et al. The framework topology of zeolite beta. Zeolites 8(6) (1988): 446-452.

[35] Forzatti, P. and Lietti, L. Catalyst deactivation. Catalysis Today 52(2) (1999): 165-181.

[36] Bartholomew, C.H. Mechanisms of catalyst deactivation. Applied Catalysis A: General 212(1) (2001): 17-60.

[37] Peng, J., Li, X., Tang, C., and Bai, W. Barium sulphate catalyzed dehydration of lactic acid to acrylic acid. Green Chem. 16(1) (2014): 108-111.

[38] Tang, C., et al. Strontium pyrophosphate modified by phosphoric acid for the dehydration of lactic acid to acrylic acid. RSC Advances 4(55) (2014): 28875.

[39] Yan, B., Tao, L.-Z., Liang, Y., and Xu, B.-Q. Sustainable Production of Acrylic Acid: Catalytic Performance of Hydroxyapatites for Gas-Phase Dehydration of Lactic Acid. ACS Catalysis 4(6) (2014): 1931-1943.

[40] Wang, H., Yu, D., Sun, P., Yan, J., Wang, Y., and Huang, H. Rare earth metal modified NaY: Structure and catalytic performance for lactic acid dehydration to acrylic acid. Catalysis Communications 9(9) (2008): 1799-1803.

[41] Zhang, J., et al. Na2HPO4-modified NaY nanocrystallites: efficient catalyst for acrylic acid production through lactic acid dehydration. Catalysis Science & Technology 4(5) (2014): 1376.

[42] Yan, B., Tao, L.Z., Liang, Y., and Xu, B.Q. Sustainable production of acrylic acid: alkali-ion exchanged beta zeolite for gas-phase dehydration of lactic acid. ChemSusChem 7(6) (2014): 1568-78.

[43] Yan, B., Mahmood, A., Liang, Y., and Xu, B.-Q. Sustainable production of acrylic acid: Rb + - and Cs + -exchanged Beta zeolite catalysts for catalytic gas-phase dehydration of lactic acid. Catalysis Today 269 (2016): 65-73.

[44] Groen, J., Peffer, L.A., Moulijn, J., and Pérez-Ramí, J. On the introduction of intracrystalline mesoporosity in zeolites upon desilication in alkaline medium. Microporous and mesoporous materials 69(1) (2004): 29-34.

[45] Maki-Arvela, P., Simakova, I.L., Salmi, T., and Murzin, D.Y. Production of lactic acid/lactates from biomass and their catalytic transformations to commodities. Chem Rev 114(3) (2013): 1909-1971.

[46] Wong, K.M., Ramli, Z., and Nur, H. Effect of loaded alkali metals on the structural, basicity and catalytic activity of zeolite beta. Jurnal Teknologi 42(1) (2012): 43–55.

[47] San-José-Alonso, D., Juan-Juan, J., Illán-Gómez, M., and Román-Martínez, M. Ni, Co and bimetallic Ni–Co catalysts for the dry reforming of methane. Applied Catalysis A: General 371(1) (2009): 54-59.

[48] Pompeo, F., Nichio, N.N., González, M.G., and Montes, M. Characterization of Ni/SiO 2 and Ni/Li-SiO 2 catalysts for methane dry reforming. Catalysis Today 107 (2005): 856-862.

[49] Wannaborworn, M., Praserthdam, P., and Jongsomjit, B. A comparative study of solvothermal and sol-gel-derived nanocrystalline alumina catalysts for ethanol dehydration. Journal of Nanomaterials 2015 (2015).

APPENDIX

APPENDIX A.

CALCULATION OF CATALYST PREPARATION

The weight percent of potassium loading on H-beta zeolite catalyst by incipient wetness impregnation method can be calculated follow

1. Calculation of potassium loading

- A : Weight percent loading of potassium on H-beta zeolite catalyst
- B : The weight of H-beta zeolite catalyst
- V : The pore volume (mL) per gram of H-beta zeolite catalyst
- 101.10 g/mole : The molecular weight of potassium nitrate
- 39.0983 g/mole : The molecular weight of potassium
- K : The potassium (K) that required
- Y : The potassium nitrate (KNO_3) that required

The potassium that required for solute in deionized water volume BV ml

$$K = \frac{\text{A g of Potassium (K)}}{\text{(100 - A) g of H-beta zeolite}} \text{ x B g of H-beta zeolite}$$

The potassium nitrate required for solute in deionized water volume BV ml

$$Y = \frac{\text{A. B g of Potassium (K)}}{\text{(100 - A)}} \text{ x } \frac{\text{101.10 g Potassium nitrate } (KNO_3)}{\text{39.0983 g Potassium (K)}}$$

2. Example: The potassium nitrate that required for H-beta zeolite40-6 wt. %K

- 6 weight percent loading of potassium on H-beta zeolite40 catalyst
- 2 g of H-beta zeolite40 catalyst
- pore volume of H-beta zeolite40 have 0.8 mL/g
- The volume of deionized water that required is 1.6 mL

The potassium nitrate required for solute in deionized water volume 1.6 ml

$$Y = \frac{6 \text{ x } 2 \text{ g (K)}}{(100 - 6)} \text{ x } \frac{101.10 \text{ g } (KNO_3)}{39.0983 \text{ g (K)}} = 0.3301 \text{ g } (KNO_3)$$

APPENDIX B.

CALCULATION OF THE ACID SITE OF CATALYST

The acid site on surface catalyst of H-beta zeolite that modified with potassium were characterized by ammonia temperature program desorption (NH_3-TPD) that can be calculated from the NH_3-TPD profile as the following step

1. Calibration curve between area and amount of ammonia

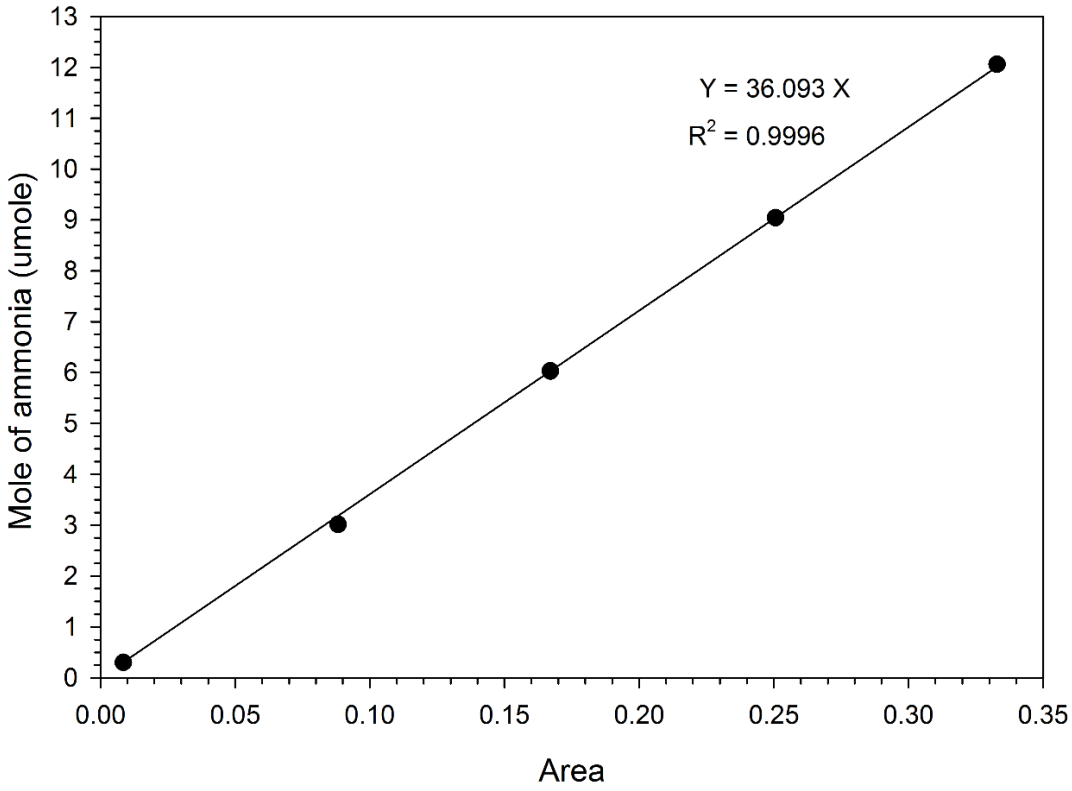

Figure B. 1 the calibration curve of ammonia from Micromeritics Chemisorp 2750

2. Given

- A : the area NH_3-TPD of profile of modified H-beta zeolite catalyst
- B : the amount of modified H-beta zeolite catalyst
- C : the acidity of catalyst in micromole NH_3 per gram catalyst

The acidity of all catalysts can be calculated from

$$\text{The acidity of catalyst (C)} = \frac{36.093 \times A}{B} \text{ umole } NH_3 \text{/g catalyst}$$

APPENDIX C.

CALCULATION OF THE BASIC SITE OF CATALYST

The basic site on surface catalyst of H-beta zeolite that modified with potassium were characterized by carbondioxide temperature program desorption (CO_2-TPD) that can be calculated from the CO_2-TPD profile as the following step

1. Calibration curve between area and amount of carbondioxide

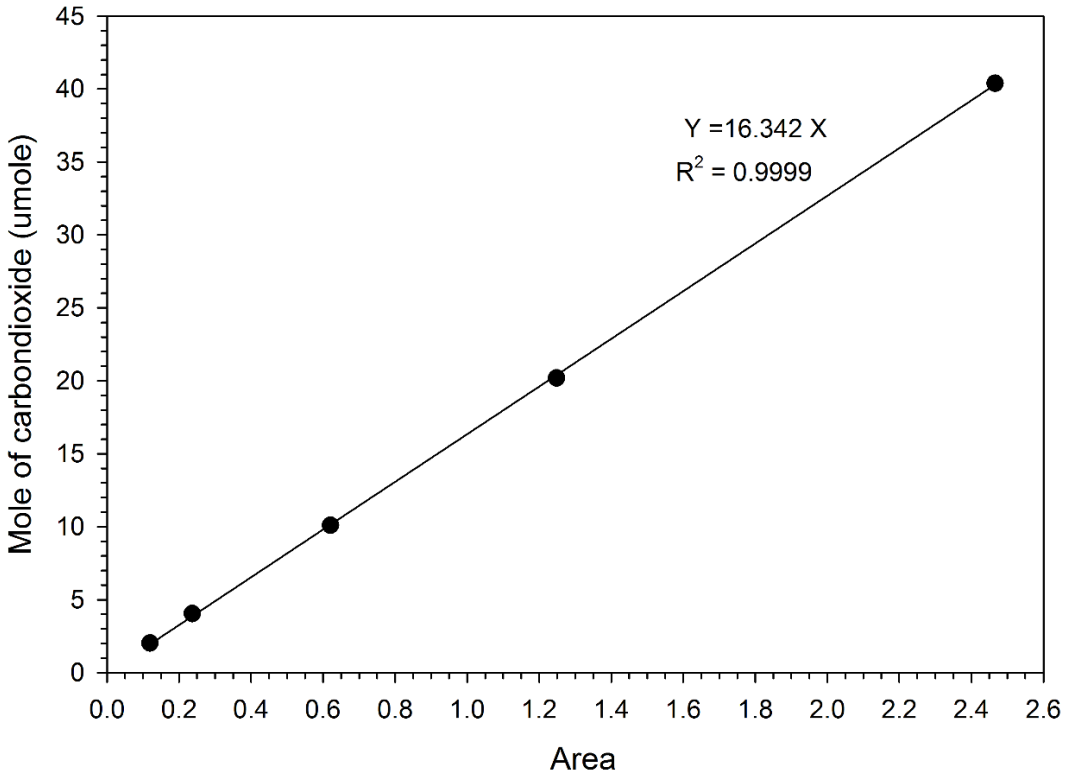

Figure C. 1 the calibration curve of carbondioxide from Micromeritics Chemisorp 2750

2. Given

- A : the area CO_2-TPD of profile of modified H-beta zeolite catalyst
- B : the amount of modified H-beta zeolite catalyst
- C : the basicity of catalyst in micromole CO_2 per gram catalyst

The basicity of all catalysts can be calculated from

$$\text{The acidity of catalyst} = \frac{16.342 \times A}{B} \text{ umole } CO_2/\text{g catalyst}$$

APPENDIX D.

CALIBRATION CURVE OF REAGENT

The composition of reactant and product in dehydration of lactic acid to acrylic acid reaction over H-beta zeolite catalyst that was modified by potassium. The main reactant is lactic acid, the main product is acrylic acid and the other product include 2, 3-pentanedione, acetaldehyde and propionic acid.

The component of reactant and product was analyzed by gas chromatography Shimadzu model 14-B with flame ionization detector (FID) and DB-WAX Ul column. The condition that was used in gas chromatography Shimadzu model 14-B.

The calibration curves exhibit area and mole of gas in x-axis and y-axis, respectively. The curve of lactic acid, acrylic acid, acetaldehyde, propionic acid and 2,3-pentanedione are shown in Fig. D1 to D5.

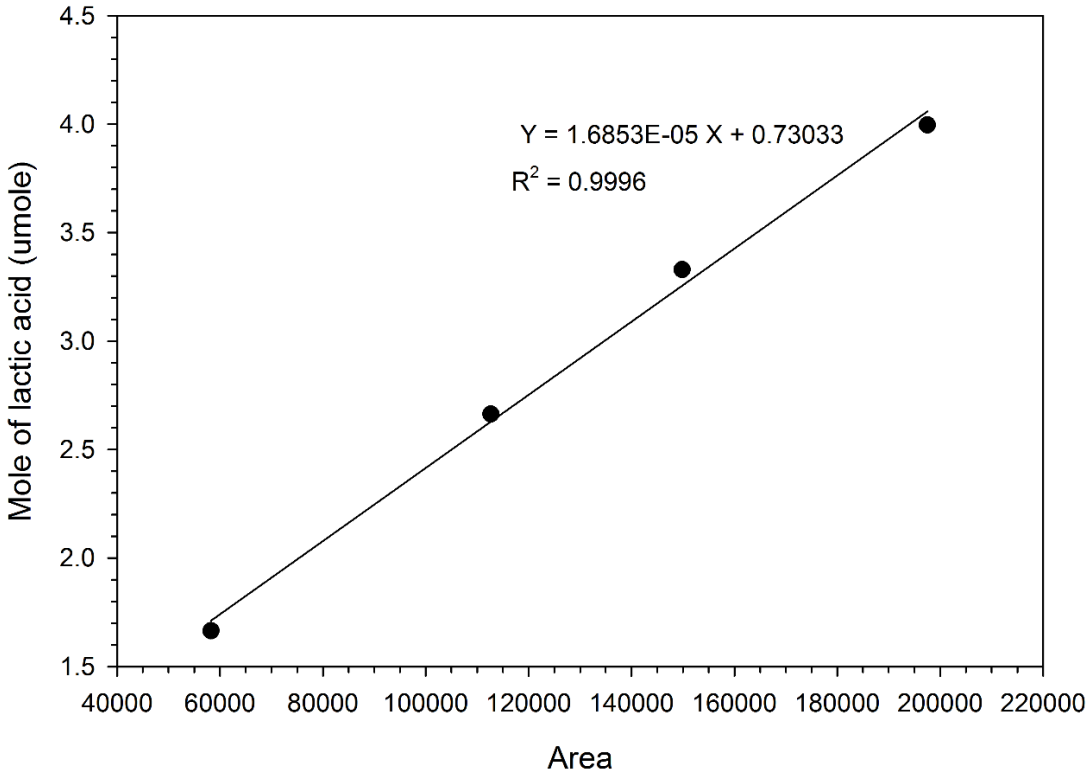

Figure D. 1 The calibration curve of lactic acid

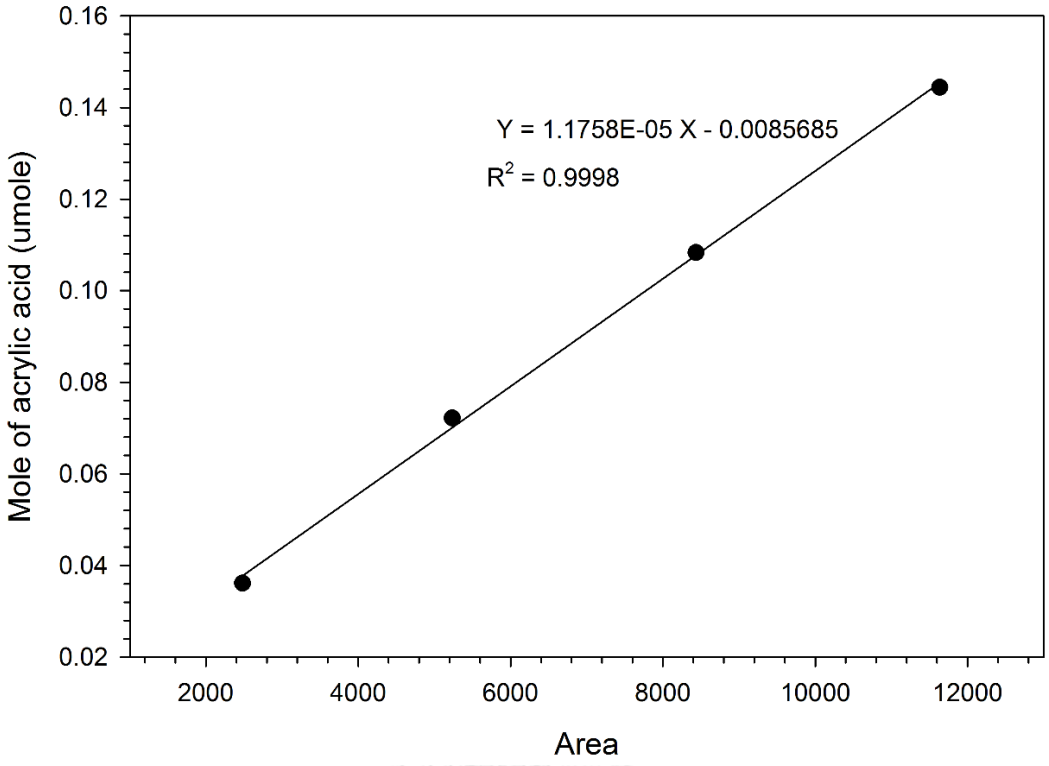

Figure D. 2 The calibration curve of acrylic acid

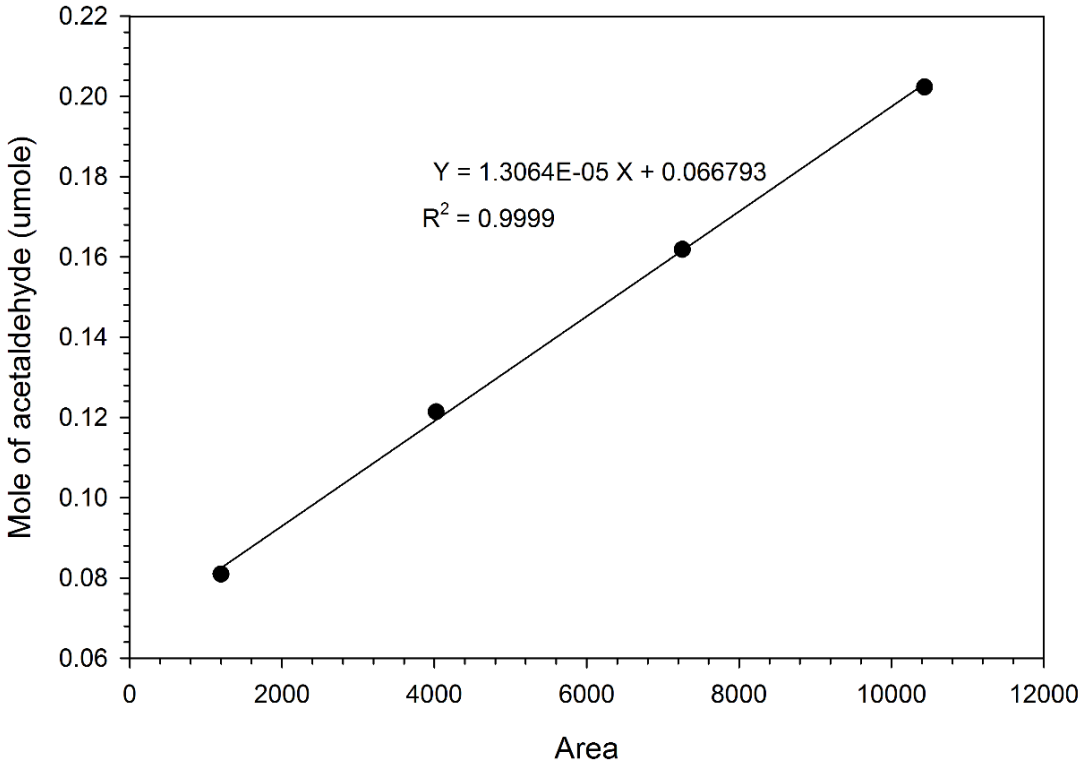

Figure D. 3 The calibration curve of acetaldehyde

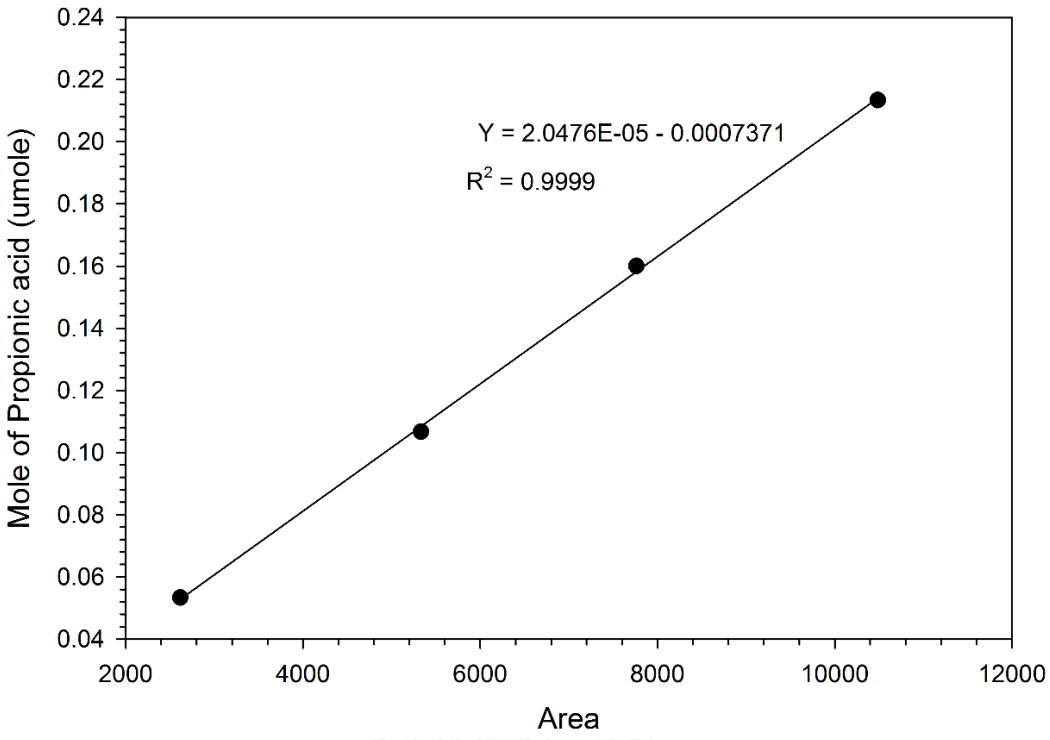

Figure D. 4 The calibration curve of propionic acid

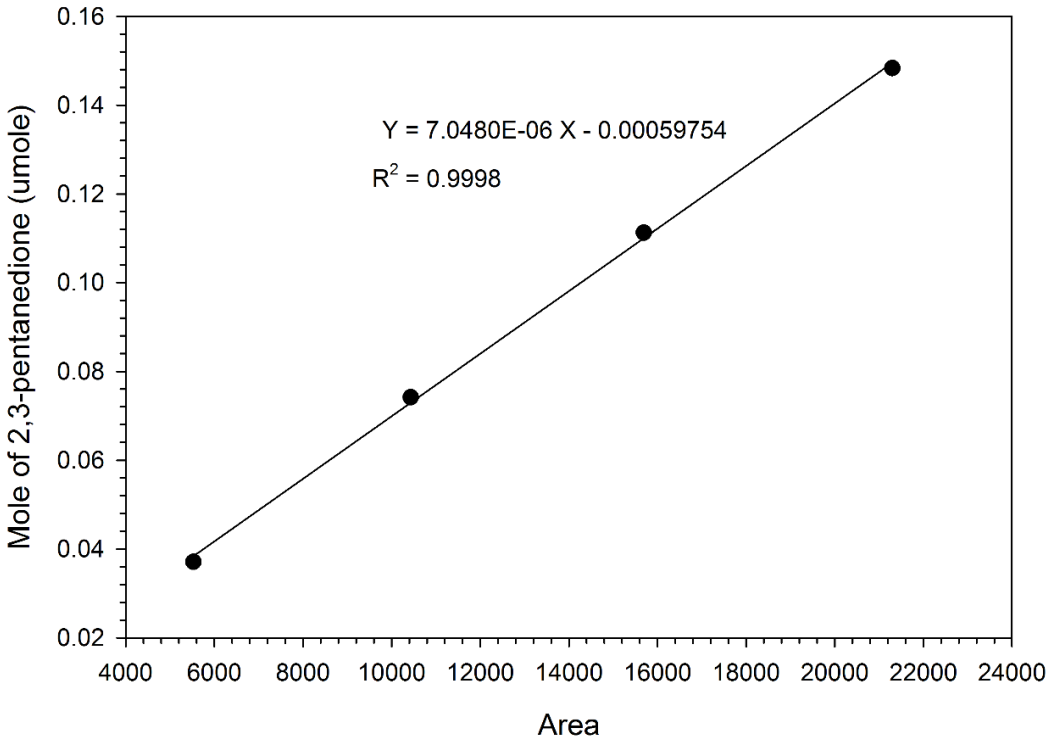

Figure D. 5 The calibration curve of 2,3-pentanedione

APPENDIX E.

CALCULATION OF CONVERTION AND SELECTIVITY

The catalytic performance for the dehydration of lactic acid to acrylic acid was evaluated in term of lactic acid conversion and acrylic acid selectivity.

1. Calculation of lactic acid conversion

The lactic acid conversion is defined as mole of lactic acid converted per mole of lactic acid in feed as follow.

$$\text{Lactic acid convertion (\%)} = \frac{\text{Area of lactic acid in feed - Area of lactic acid in product}}{\text{Area of lactic acid in feed}} \times 100$$

2. Calculation of products selectivity

The products selectivity are defined as mole of products generated per total mole of product that generated that content acrylic acid, acetaldehyde, propionic acid and 2,3-pentanedione as follow.

$$\text{Acrylic acid selectivity (\%)} = \frac{\text{Mole of acrylic acid in product}}{\text{Total mole of products}} \times 100$$

$$\text{Acetaldehyde selectivity (\%)} = \frac{\text{Mole of acetaldehyde in product}}{\text{Total mole of products}} \times 100$$

$$\text{Propionic acid selectivity (\%)} = \frac{\text{Mole of propionic acid in product}}{\text{Total mole of products}} \times 100$$

$$\text{2, 3-propanedione selectivity (\%)} = \frac{\text{Mole of 2, 3 propanedione in product}}{\text{Total mole of products}} \times 100$$

Where the total mole of products are the summation of mole of acrylic acid, acetaldehyde, propionic acid and 2, 3 propanedione, respectively.

VITA

Mr. Weerapong Phochaisang was born on January 3th, 1991 in Kalasin province, Thailand. He finished high school education from Ratchaborikanukroh School in 2010 and graduated his bachelor's degree in Petrochemicals and Polymeric Materials Engineering from Faculty of Engineering and Industrial Technology, Silpakorn University of Sanam Chandra Palac Campus, Nakornpathom province, Thailand in April 2014. He continued his study for Master's degree of Chemical Engineering, Department of Chemical Engineering, Faculty of Engineering at Chulalongkorn University in Bangkok, Thailand since 2014 and joined the center of excellence on catalysis and catalytic reaction engineering for his research.